LIST OF APPENDICES

Appendix	Page No.
Appendix A	xvii-xxvi
Appendix B	xxvii-xxx
Appendix C	xxxi-xxxiv
Appendix D	xxxv-xlvii
Appendix E	xlviii-lix

Appendix A

Effects of water content and oil on physicochemical and microenvironmental properties of mixed surfactant microemulsions

1. Fluorescence lifetime measurements

For time-resolved fluorescence measurements, the instrument employs Stroboscopic Technique (Strobe).The strobe technique is very much similar to the time-correlated single photon counting technique (TCSPC) in respect of measurement and data analysis. The differences are mainly in hardware component, wherein different detection electronic components and pulsed light sources were used [1-3]. In the present report, two curves are considered at the measured wavelength (i.e., at 450 nm using 310 nano LED as the light source) viz. the instrument response function (IRF) and the decay curve of probe molecules, 7-hydroxycoumarin (10^{-5} mol dm^{-3}). IRF is acquired from a non-fluorescent scattering solution (herein, LudoxAM-30 colloidal silica, 30 wt% suspension in water) held in a 1 cm path length quartz cell. The lifetime values of probe molecules are then obtained by convoluting the IRF with a model function and then comparing the result with the experimental decay. This is done by an iterative numerical procedure until the best agreement with the experimental decay curve is achieved (e.g., a single or double exponential decay). Analysis has been made by Felix GX (version 2.0) software. Goodness of the fluorescence lifetime data fits in the curves, as adjudged by χ^2 value (less than 1.10) and with a residuals trace, which is fully symmetrical about the zero axes. A representative illustration has been shown in Fig. S1.

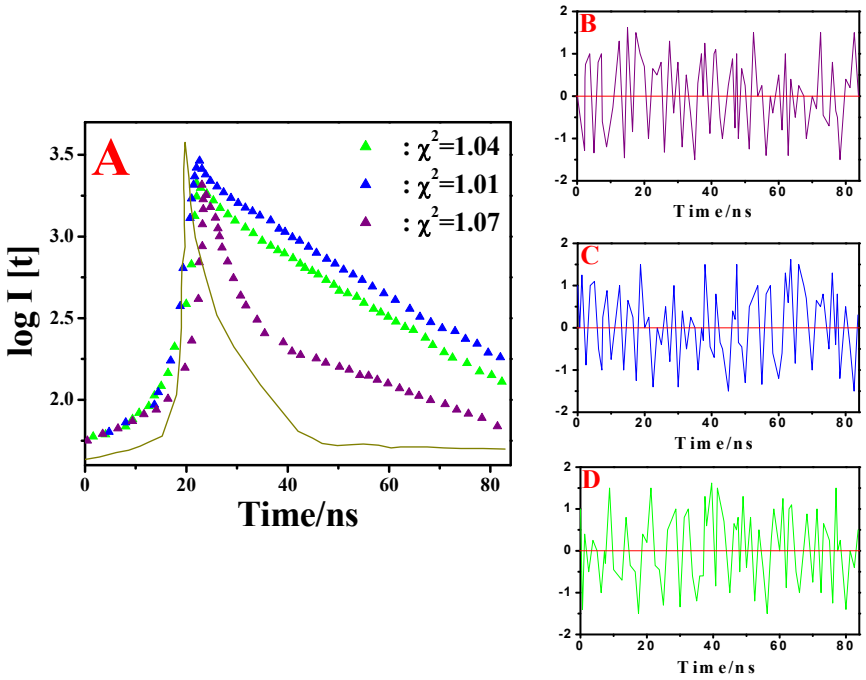

Fig. S1. Representative fluorescence decay (A) of HCM (λ_{ex}= 310 nm) in water/(C_{16}TAB + $C_{16}E_{20}$, 1:1)/Bu/Hp microemulsions as a function of molar ratio of water to surfactant, ω with corresponding χ^2 values and residual traces. Specifications: Solid line indicates system response (IRF), purple triangle; ω = 10 (residual trace; B), blue triangle; ω = 40 (residual trace; C), green triangle; ω = 50 (residual trace; D).

2. Phase Behavior of mixed surfactant microemulsions

Phase diagrams of pseudo-quaternary systems composed of surfactant(s), cosurfactant, oil and water at a constant temperature and pressure can be best represented with the help of three-dimensional Gibbs tetrahedron with four components as the four apexes. In the present study, the phase diagrams are constructed in a simple two-dimensional Gibbs triangle after cutting the Gibbs tetrahedron along a constant surfactant, cosurfactant mass ratio (1:2) plane. The compositions in the phase diagrams are represented in weight fraction.

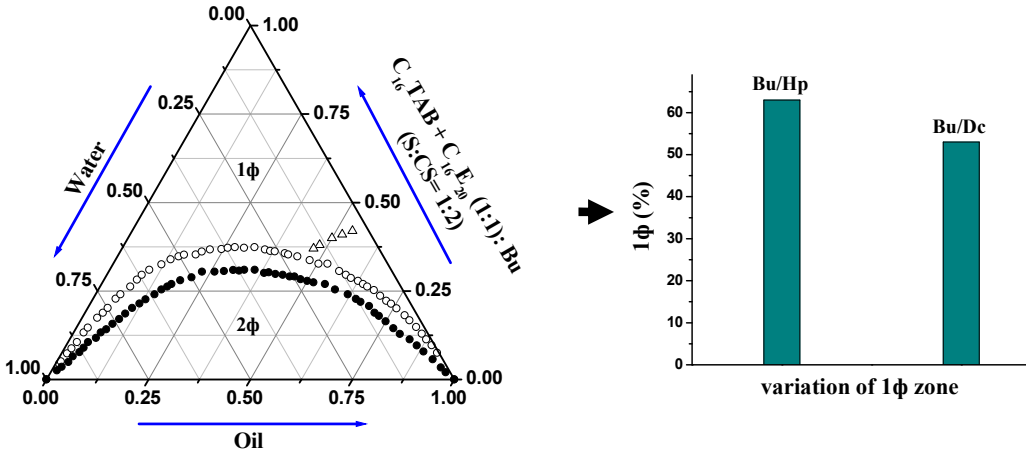

Fig. S2. The pseudo-ternary phase diagram of equimolar (1:1) mixed surfactant microemulsion system [water/(C_{16}TAB + $C_{16}E_{20}$)/Bu/Hp or, Dc] indicates the formation of a significant single phase (1ϕ) region in mixed surfactant, cosurfactant mass ratio (1: 2) and oil mixtures at 303K. Area marks: microemulsion zone (1ϕ); turbid zone (2ϕ). Phase boundary composition: filled circle (●); Hp, open circle (○); Dc. Open triangles (Δ) in 1ϕ zone indicates a typical dilution pathway (ω= 10→50). Histogram indicates the variation of 1ϕ zone with oil (Hp/Dc) for the same system. Points (Δ) in the phase diagram represent the compositions where further characterization was done. Appearance of viscous and other phases along the [surfactant(s): cosurfactant/water]-oil axis have not been shown for simplicity.

Fig. S2 represents the pseudo-ternary phase diagram of equimolar (1:1) mixed surfactant microemulsion system [water/(C_{16}TAB + $C_{16}E_{20}$)/Bu/Hp (or, Dc)] at 303K. Each pseudo-ternary phase diagram comprises of a single phase (1ϕ) clear microemulsion region and a two phase (2ϕ) turbid region. The extreme corners of the polar component (herein, water) and oil component correspond to oil-in-water and water-in-oil microemulsions, respectively. In the present system, the oil rich regions, i.e., water-in-oil microemulsions were examined for other set of experiments. Areas under the clear and turbid regions were calculated by weighing the individual components in the pseudo-ternary phase diagram. However, the construction of phase diagram for pseudo-ternary microemulsion systems are essential from fundamental as well as application point of

view [4]. During the determination of single phase (1ϕ) clear microemulsion region, viscous and biphasic regions are appeared along the water-oil axis. This is not shown in the Figures for the sake of simplicity. Generally, phase behavior of a microemulsion system determines its microstructure. It is well established that the phase behavior and the microstructure of microemulsions are dependent on two interfacial parameters, namely the spontaneous film curvature (H^0) (the curvature that the amphiphilic film would like to attain) and the elasticity of the amphiphilic film [5]. Further, the H^0 can be affected by the nature and composition of amphiphile(s) [6]. In the present report, equimolar (1:1) mixed surfactant has been used as tuning parameter to change H^0 vis-à-vis to increase the flexibility of the surfactant film [7-9]. Actually, POE chains of the nonionic surfactant ($C_{16}E_{20}$), extend its polar head groups within the water pools and lead to produce more flexible films, resulting to curve the interface away from the water pool [10]. Furthermore, cosurfactant used as a fourth component in microemulsion, can easily affect interfacial properties of microemulsions. Increasing alcohol chain length often increases the interfacial rigidity vis-à-vis curvature of the interface and vice versa [11]. However, the medium chain alcohol (herein, Bu) used in the present report, is known for increasing fluidity with decreasing the H^o [12]. Additionally, the formation of w/o microemulsion in 1ϕ region also reflects the effect of variation of oil chain length (Hp or Dc). However, when one analyses the results in terms of the variation of % area under the clear region with the variation of oil chain length, it can be observed from Fig. S2 (histogram) that % area under the clear region are higher for Hp stabilized systems compared to Dc stabilized systems. Similar observation was reported earlier by Mitra and Paul [13] for water/C_{16}TAB or Brij-58/Bu/Hp or Dc microemulsion systems.

3. Conductance measurements

It is known that electrical conductivity measurement can be used to predict qualitatively the interaction between droplets and thus the stability of microemulsion. For example, appearance of an electrical percolation process indicates the existence of large attractive interaction between droplets [14, 15]. Fig. S3 represents the electrical conductivity (σ) of water/(C_{16}TAB + $C_{16}E_{20}$)/Bu/Hp (or Dc) microemulsions as a function of water content (ω) at equimolar composition (1:1) of mixed surfactant and at constant temperature of 303K. The mixed surfactant and cosurfactant mass ratio (1:2) were fixed throughout the experiment. It has been observed from Fig. S3 that, the conductance gradually increases with increase in water content (ω = 10→50) in both oils (Hp or Dc) for the mixed systems. Such an increase in conductivity with increase in ω may be due to both the progressive increase in the hydration of a POE chain of the nonionic surfactant ($C_{16}E_{20}$) and the 'transient fusion-mass transfer-fission' process involving in cationic surfactant (C_{16}TAB), because of the transfer of ions between adhering droplets in these w/o microemulsion systems [6, 15, 16]. However, a nonlinear sharp increase in conductivity has been observed above ω ~ 40 in both oils, as evidenced from Fig. S3. The sharp enhancement in conductivity at higher water content (ω ~ 40) may be due to volume-induced percolation in conductance in the present system [14]. Such percolation shows that the interface of the droplets is fluid enough to coalesce during the collisions followed by material exchange and fusion. Percolation signifies the increase in droplet size, attractive interaction among droplets and exchange rate of materials between the droplets with the addition of water [15, 17, 18]. Similar observation was reported by Li et al. [19] and Zhang et al. [20] for water/TX-100/Bu/Hp and water/AOT/Bu/IPM w/o microemulsion systems, respectively. The variation in droplet size with water content, as reflected from DLS measurements (discussed in Sec. 3.2), corroborates well with the features obtained conductance measurements. Hydrodynamic diameter obtained from DLS measurements indicates droplet-droplet interaction at higher water content (ω ≥ 30), which supports the percolation behavior in conductance data at ω ~ 40. Similar result was also reported by Lemyre et al. [21] for water/Igepal CO-520 (polyoxyethylene (5) nonylphenyl ether)/cyclohexane microemulsion system.

However, from Fig. S3 it has also been observed that, Dc stabilized system produces higher conductivity than Hp stabilized system. This can be explained in the following way. It was reported earlier that, oil penetration into the surfactant tail region is smaller for longer chain hydrocarbon oils (herein, Dc) [22, 23], which causes a decrease in the spontaneous curvature of surfactant layer in comparison to smaller chain hydrocarbon oils (herein, Hp) and favors the formation of larger droplet in Dc continuum. On the other hand, the large oil penetration in Hp derived systems swells the aliphatic layer of the surfactant film to a greater extent, causing a higher spreading pressure at the surfactant tail/oil interface. Consequently, smaller droplets are formed with higher surface curvatures [23]. The increase in the molar mass of the hydrocarbon oil (Hp→Dc) decreases the density of the continuous phase enabling the interacting droplets to approach towards each other more easily for mass transfer [24]. Consequently, the longer chain oil penetrates less into the interface causing greater inter-droplet attraction. Hence, both inter-droplet attraction and the exchange of mass increase with increase in apolar solvent chain length in w/o microemulsion systems. All these factors lead to higher conductivity in Dc-derived system compared to the Hp-derived system.

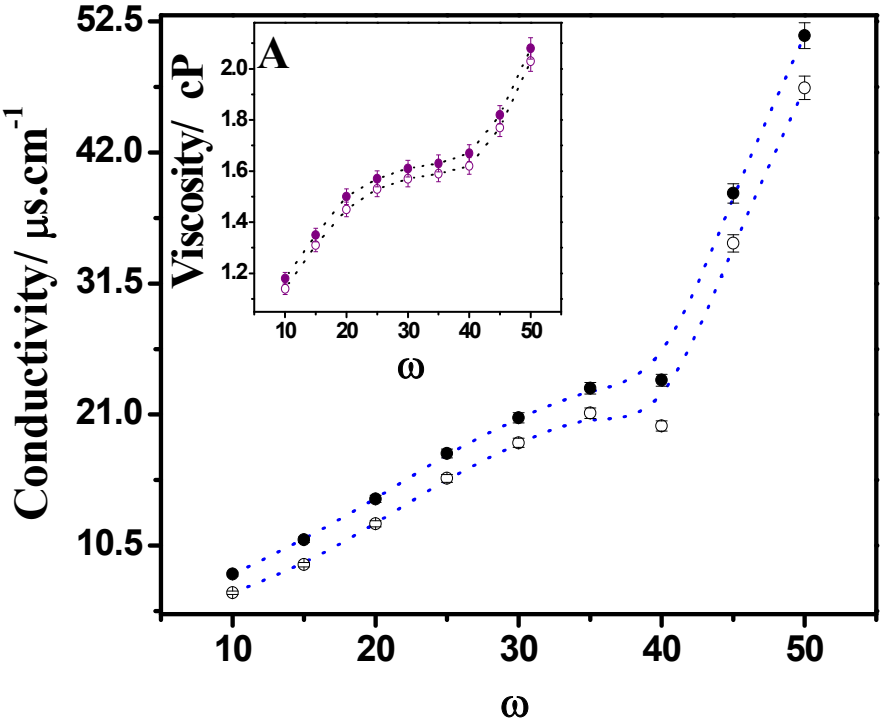

Fig. S3. Dependence of the electrical conductivity (σ) of water/(C_{16}TAB + $C_{16}E_{20}$, 1:1)/Bu/Hp (or Dc) microemulsions as a function of molar ratio of water to surfactant (ω) at a constant temperature of 303K. Open circle: Bu/Hp, filled circle: Bu/Dc. **Inset A:** Viscosity (η) vs. ω profile (open/filled circle: Hp/Dc). Dotted lines are guides to the eye.

4. Viscosity measurements

Further, the microstructural features of w/o mixed surfactant microemulsions have been investigated by viscosity measurement. Generally, the size of the dispersed droplets, the droplet-droplet interaction and the viscosity of the continuum medium are determined from the viscosity measurements [25-27]. Herein, same set of compositions and temperature (303K) were used for viscosity measurements as employed for conductance studies. It has been observed that, the

viscosity of the mixed microemulsions gradually increases with increase in ω (= 10→50) (Fig. S3, inset A). These systems exhibit Newtonian behavior along the experimental path. The absence of maximum in viscosity with increasing ω rules out the presence of any structural transition from w/o to o/w, and supports the formation of w/o microemulsion at the studied composition range of the present system [25, 26]. It is well known that increase in viscosity of w/o microemulsions emerges from increase in size of the dispersed water droplets which, enhances the attractive interaction between droplets in continuous phase at higher level of hydration [26-28]. It is noteworthy to mention that both the transport parameters viz., conductivity and viscosity are found to be influenced by the droplet size and attractive interdroplet interaction of microemulsion systems [26, 28]. Consequently, viscosity trend upon varying ω shows clearly parallel nature with that of conductivity. However, less penetration of oil into the surfactant film with increasing oil chain length (Hp→Dc) results in a more flexible interface and a greater natural radius than that of short chain oils. The attractive interactions between the droplets are thus increased due to sticky collisions, which results in increase of the viscosity in Dc continuum [23].

Table S1. Basic data of fluorescence lifetime of HCM as a function of water content (ω) in water/(C_{16}TAB + $C_{16}E_{20,}$ 1:1)/Bu/Hp (or Dc) microemulsions at a constant temperature of 303 K.

ω	Shorter Lifespan	Longer Lifespan
10	2.56 (2.76)	36.28 (37.51)
20	3.97 (4.21)	36.39 (37.62)
30	4.15 (4.34)	----
40	4.95 (5.09)	----
50	4.39 (4.57)	----

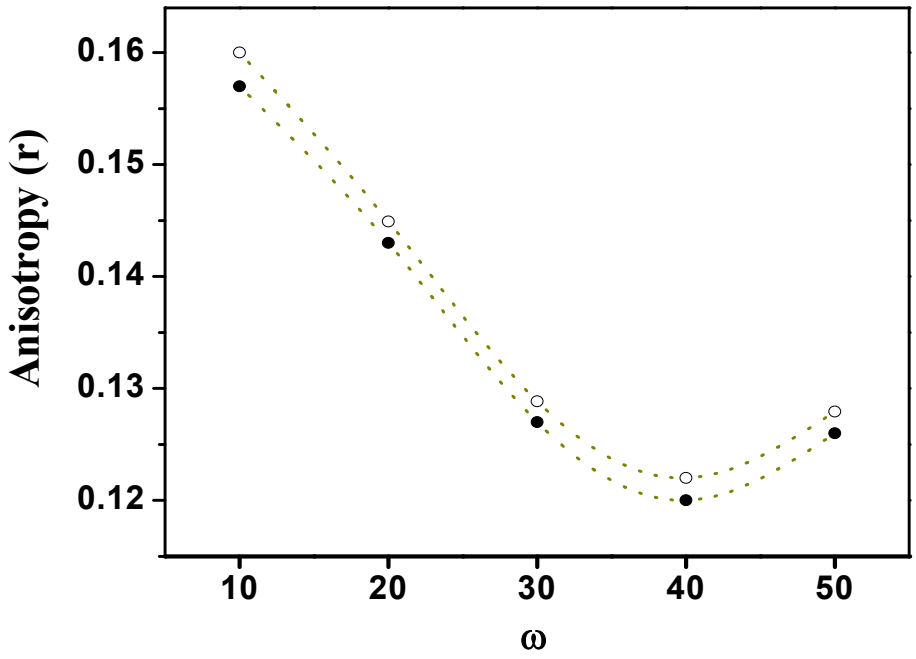

Fig. S4. Steady state fluorescence anisotropy (r) as a function of molar ratio of water to surfactant (ω) in water/(C_{16}TAB: $C_{16}E_{20,}$ 1:1)/Bu/Hp (or Dc) microemulsions at a constant temperature of 303K, Open circle: Bu/Hp, filled circle: Bu/Dc, Dotted lines are guide to the eye (λ_{ex} of Eosin Y= 500 nm).

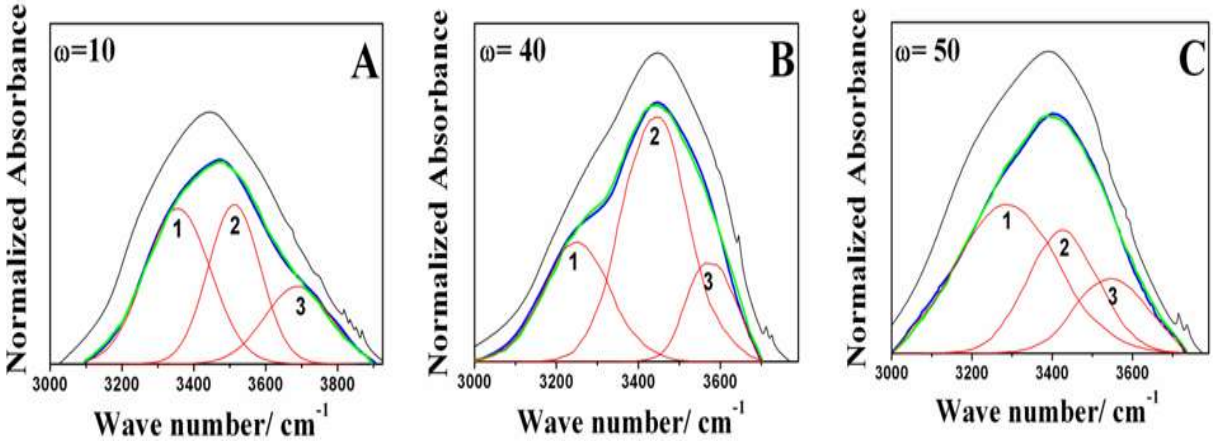

Fig. S5. Representative normalized (normalized to intensity of 1.0) FTIR (A, B, C) spectra of O-H band for w/o mixed microemulsion system [water/(C_{16}TAB + $C_{16}E_{20,}$ 1:1)/Bu/Hp] with the variation of molar ratio of water to surfactant, ω (= 10→50). Specification: Black curve; original spectra, Blue curve; spectra after subtraction of OH stretching vibration at the Bu site, green curve; overall fitted curve and red curve; deconvoluted curves (*1: bulk water; 2: bound water; 3: trapped water*) respectively.

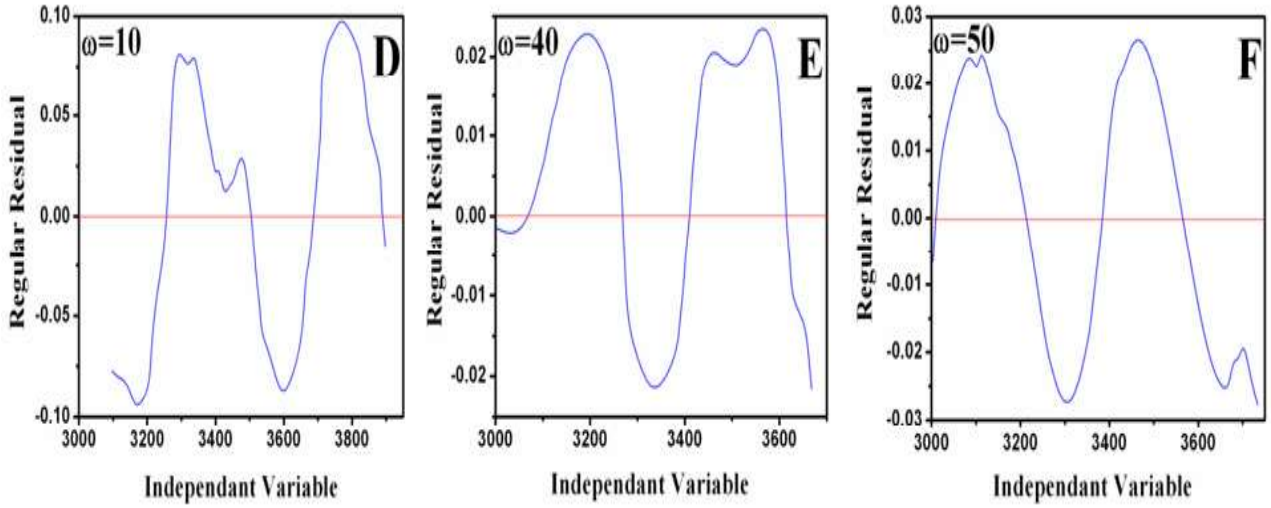

Fig. S6. The residuals graphs of the deconvolution of FTIR (A, B, C) spectra of O-H band for (w/o) mixed microemulsion system [water/(C_{16}TAB + $C_{16}E_{20,}$ 1:1)/Bu/Hp] with the variation of ω (= 10→50).

Table S2. Statistical parameters (degrees of freedom and coefficient of determination), as evaluated form deconvolution software (Origin Lab), about the goodness of fit of curves with the variation of ω (= 10→50).

ω	Degrees of freedom	coefficient of determination (R^2)	Reduced χ^2
10	645	0.99	0.88
20	681	0.99	0.89
30	717	0.99	0.87
40	789	0.98	0.88
50	750	0.99	0.89

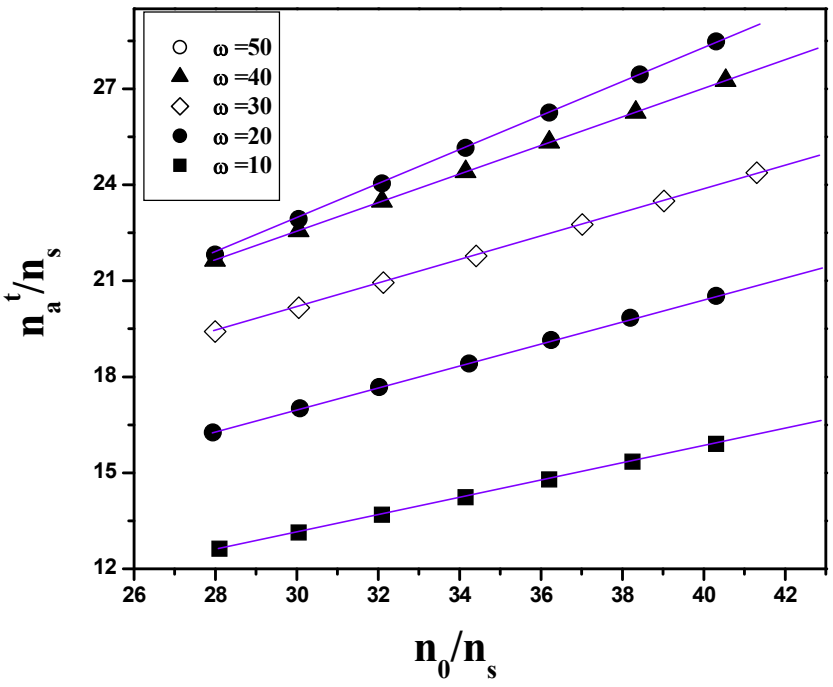

Fig. S7. Plots of n_a^t / n_s against n_0 / n_s according to Eq. (3) for w/o microemulsion systems comprising equimolar (1:1) mixed surfactant (C_{16}TAB and $C_{16}E_{20}$) (0.5 mmol) and decane (14.0 mmol) stabilized by Bu with different ω (= 10→50) at constant temperature (303K).

References

[1] A.S. Mukhopadhyay, S.S. Maity, A. Roy, D. Chattopadhyay, K.S. Ghosh, S. Dasgupta, S. Ghosh, Biochimie. 92 (2010) 136.
[2] S. Paul, A.K. Panda, Colloids Surf. A 419 (2013) 113.
[3] M. Chakraborty, A.K. Panda, Spect. Acta. Part A 81 (2011) 458.
[4] B.K. Paul, S.P. Moulik, Curr. Sci. 80 (2001) 990.
[5] A. Yaghmur, A. Aserin, N. Garti, Colloids Surf. A 209 (2002) 71.
[6] S.K. Mehta, G. Kaur, R. Mutneja, K.K. Bhasin, J. Colloid Interface Sci. 338 (2009) 542.
[7] M. Kahlweit, B. Faulhaber, G. Busse, Langmuir 10 (1994) 2528.
[8] C.V. Corswant, S. Engstrom, O. Soderman, Langmuir 13 (1997) 5061.
[9] A. Dogra, A.K. Rakshit, J. Phys. Chem. B 108 (2004) 10053.
[10] L.M.M. Nazario, J.P.S.G. Crespo, J.F. Holzwarth, T.A. Hatton, Langmuir 16 (2000) 5892.
[11] A. Bumajdad, J. Eastoe, R.K. Heenan, Langmuir 19 (2003) 7219.
[12] M. Kahlweit, G. Busse, B. Faulhaber, Langmuir 11 (1995) 1576.
[13] R.K. Mitra, B.K. Paul, S.P. Moulik, J. Colloid Interface Sci. 300 (2006) 755.
[14] B.K. Paul, R.K. Mitra, S.P. Moulik, Microemulsions: Percolation of conduction and thermodynamics of droplet clustering, in: P. Somasundaran (Ed.), Encyclopedia of Surface and Colloid Science, Taylor and Francis, New York, 2006, 3927.
[15] A. Kljaji´c, M. Be˘ster-Roga˘c, S. Tro˘st, R. Zupet, S. Pejovnik, Colloids Surf. A 385 (2011) 249.
[16] K. Maiti, I. Chakraborty, S.C. Bhattacharya, A.K. Panda, S.P. Moulik, J. Phys. Chem. B 111 (2007) 14175.

[17] B.K. Paul, R.K. Mitra, J. Colloid Interface Sci. 288 (2005) 261.
[18] D. Liu, J. Ma, H. Cheng, Z. Zhao, Colloids Surf. A 148 (1999) 291.
[19] X. Li, G. He, W. Zheng, G. Xiao, Colloids Surf A. 360 (2010) 150.
[20] X. Zhang, Y. Chen, J. Liu, C. Zhao, H. Zhang, J. Phys. Chem. B 116 (2012) 3723.
[21] J-L. Lemyre, S. Lamarre, A. Beaupre, A.M. Ritcey, Langmuir 26 (2010) 10524.
[22] K. Kundu, B.K. Paul, Physicochemical investigation of biocompatible mixed surfactant reverse micelles: III. Aqueous NaCl Solubilization, J. Surfact. Deterg. 16 (2013) 865.
[23] R. Leung, D.O. Shah, J. Colloid Interface Sci. 120 (1987) 330.
[24] S.K. Hait, A. Sanyal, S.P. Moulik, J. Phys. Chem. B 106 (2002) 12642.
[25] S. Ajith, A.K. Rakshit, J. Phys. Chem. 99 (1995) 14778.
[26] R.K. Mitra, B.K. Paul, J. Colloid Interface Sci. 283 (2005) 565.
[27] M.S. Leaver, U. Olsson, Langmuir 10 (1994) 3449.
[28] R. Aveyard, B.P. Binks, S. Clarke, P.D.I. Fletcher, Prog. Colloid Polym. Sci. 79 (1989) 202.

Appendix B

Interfacial composition and characterization of a quaternary water-in-oil mixed surfactant (cationic of different alkyl chain lengths + polyoxyethylene type nonionic) microemulsions in absence and presence of inorganic salts

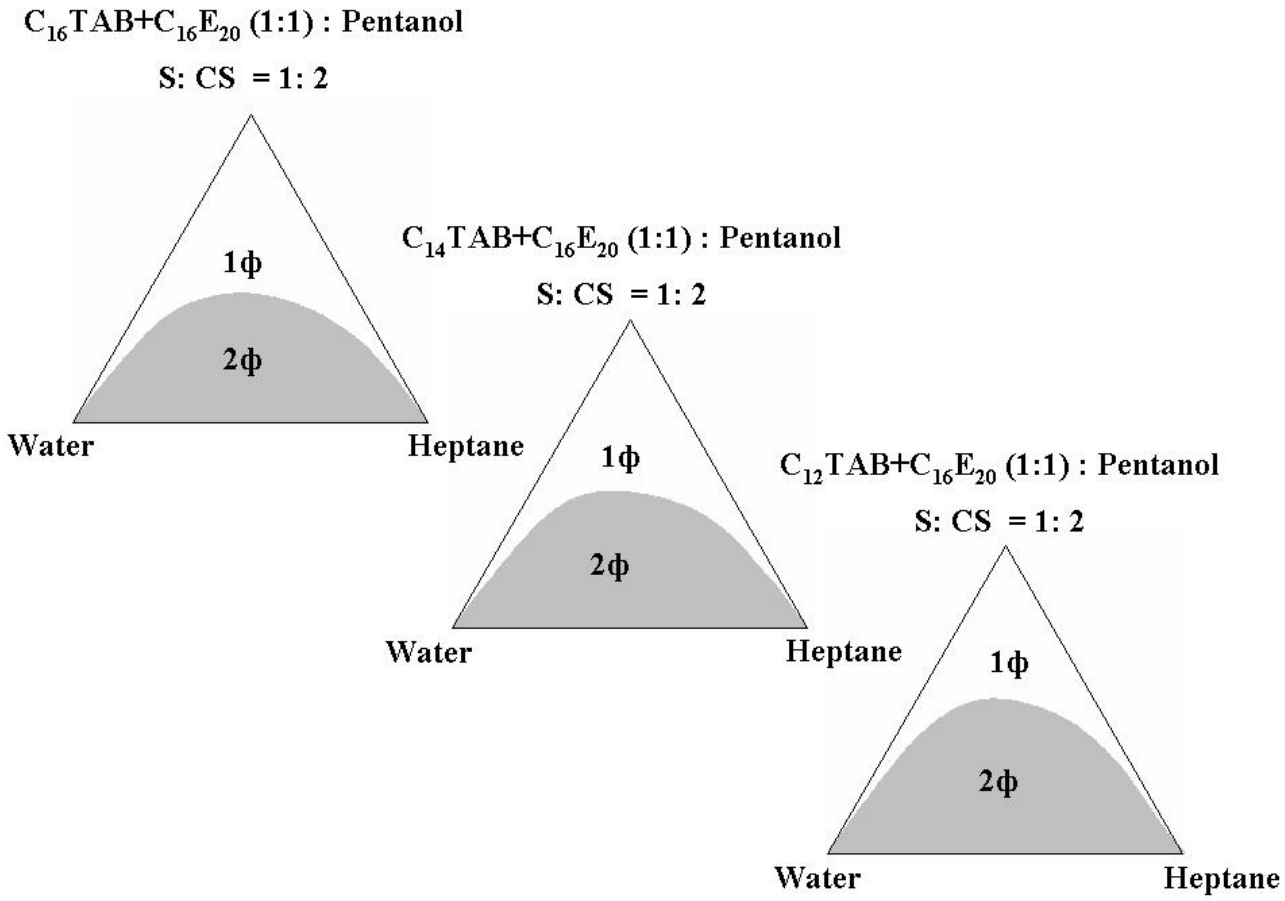

Figure S1. Representative pseudo-ternary phase diagram of equimolar (1:1) mixed surfactant ($C_nTAB + C_{16}E_{20}$, n = 16, 14, 12) microemulsion with pentanol (Pn) and hydrocarbon (Hp) oil at 303K. Area marks: unshaded, microemulsion zone (1ϕ); shaded, turbid zone (2ϕ).

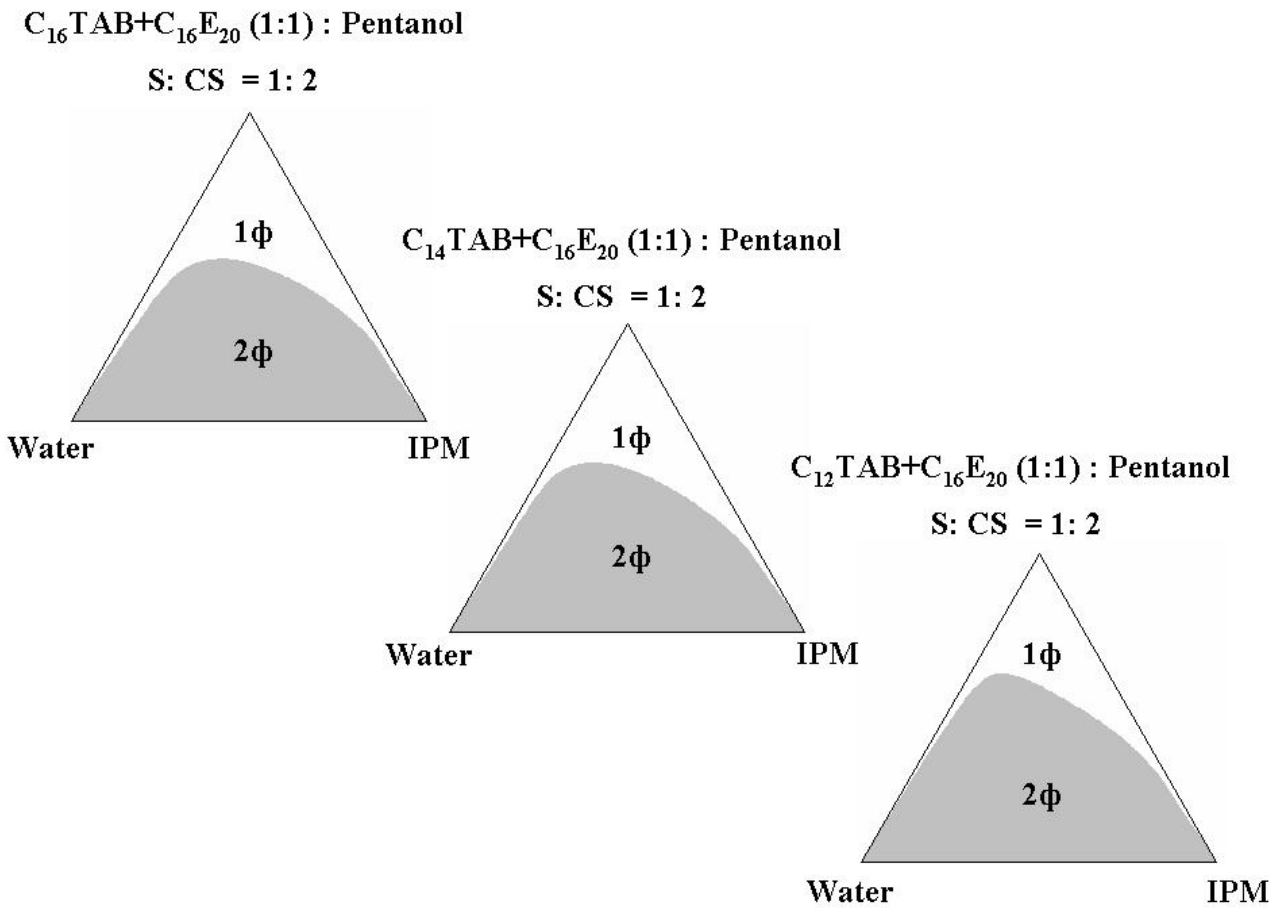

Figure S2. Representative pseudo-ternary phase diagram of equimolar (1:1) mixed surfactant ($C_nTAB + C_{16}E_{20}$, n = 16, 14, 12) microemulsion with pentanol (Pn) and IPM oil at 303K. Area marks: unshaded, microemulsion zone (1ϕ); shaded, turbid zone (2ϕ).

A. Basics of the dilution method and thermodynamics of transfer of cosurfactant from oil to the interface

For a quaternary water-in-oil microemulsion system composed of water/ surfactant/ alkanol (cosurfactant)/ oil, the solubilization of water is governed by the distribution of alkanol molecules between oil and the interface at a fixed temperature. A small amount of alkanol may remain solubilized in the aqueous phase depending on its lipophilicity. A threshold amount of alkanol is required to stabilize a water-in-oil dispersion at a fixed molar ratio of water to surfactant (ω). As a result, an appropriate distribution constant (K_d) is attained, and governs alkanol molecules distributed between the interfacial region (consisting of surfactant molecules) and the oleic phase at a fixed temperature. The stable w/o microemulsion gets disrupted when excess oil is added and the system splits up into two distinct phases. Again, a threshold amount of alkanol is necessary to restore the w/o microemulsion equilibrium. This process is repeatedly followed in the dilution experiment.

The concentrations of alkanol at the interface and in the bulk oil phase were estimated to get the distribution constant (K_d) by the dilution experiments in the light of the physicochemical rationale elaborated by Zheng et al. [1], Moulik et al. [2, 3], Paul et al. [4-6], Abuin [7], and Mehta et al. [8]. The total number of moles of the alkanol, n_a present in the stable microemulsion is given by the relation,

$$n_a = n_a^i + n_a^w + n_a^o \text{ ----------(S1)}$$

where, n_a^i, n_a^w, n_a^o are the number of moles of alkanol in the interfacial, water and oil phases respectively. Since the solubility of alkanol in the oil is constant at a given temperature, the constant k_o can be written as

$$k_o = \frac{n_a^o}{n_o} \text{ ----------(S2)}$$

where n_o is the total number of moles of oil in the system. Combining Equations S1 and S2 we get

$$n_a = n_a^i + n_a^w + k_o n_o \text{ ----------(S3)}$$

Since the moles of alkanol in the interface and in the dispersed phase (water) depend on the surfactant concentration, Equation S3 may be converted into a more convenient form by dividing throughout by total number of moles of surfactant, n_s to give

$$\frac{n_a}{n_s} = \frac{n_a^i + n_a^w}{n_s} + k_o \frac{n_o}{n_s} \text{ ----------(S4)}$$

In our experiment, negligible water solubility of Pn leads to $n_a^w \approx 0$ [8]. Thus, above equation becomes,

$$\frac{n_a}{n_s} = \frac{n_a^i}{n_s} + k_o \frac{n_o}{n_s} \text{ ----------(S5)}$$

A plot of n_a/n_s against n_o/n_s should yield the values of the slope (S) and the intercept (I). Slope (S) is actually k_o and n_a^o can be determined from Equation S2. On the other hand, n_a^i can be calculated from the intercept (I), which is equal to n_a^i/n_s.

The partition of Pn between the continuous oil phase and the interface of the droplet can be expressed in terms of the distribution constant (K_d). K_d can be calculated from the ratio of mole fraction of Pn in the interfacial composition (X_a^i) to the mole fraction of Pn in the bulk oil phase (X_a^o),

$$K_d = \frac{X_a^i}{X_a^o} = \frac{n_a^i / \left(n_a^i + n_s\right)}{n_a^o / \left(n_a^o + n_o\right)} = \frac{n_a^i \left(n_a^o + n_o\right)}{n_a^o \left(n_a^i + n_s\right)} \text{ ----------(S6)}$$

Dividing numerator and denominator by $n_a^i\, n_a^o$, and putting the values of the slope (S) and the intercept (I) from Equation S5, we get

$$K_d = \frac{\left(1 + n_o / n_a^o\right)}{\left(1 + n_s / n_a^i\right)} = \frac{\left(1 + 1/S\right)}{\left(1 + 1/I\right)} = \frac{I(1+S)}{S(1+I)} \text{ ----------(S7)}$$

The standard Gibbs free energy change of transfer ($\Delta G^0_{transfer}$) of Pn from the continuous oil phase to the interfacial region, between the water and oil, is obtained from the relation

$$\Delta G^0_{transfer} = -RT \ln K_d = -RT \ln \frac{X_a^i}{X_a^o} = -RT \ln \frac{I(1+S)}{S(1+I)} \text{ ----------(S8)}$$

References:

[1] O. Zheng, J-X. Zhao, X.-M. Fu, Langmuir, 22 (2006) 3528-3532.

[2] D. Mitra, I. Chakraborty, S.C. Bhattacharya, S.P. Moulik, S. Roy, D. Das, P.K. Das, J. Phys.Chem. B 110 (2006) 11314-11326.

[3] K. Maiti, I. Chakraborty, S.C. Bhattacharya, A.K. Panda, S.P. Moulik, J. Phys.Chem. B 111 (2007) 14175-14185.

[4] B.K. Paul, D.D. Nandy, J. Colloid Interface Sci. 316 (2007) 751-761.

[5] K. Kundu G. Guin, B.K. Paul, J. Colloid Interface Sci. 385 (2012) 96-110.

[6] K. Kundu, B.K. Paul, Colloid Polym. Sci. 291 (2013) 613.

[7] E. Abuin, E. Lissi, K. Olivares, J. Colloid Interface Sci. 276 (2004) 208-211.

[8] S.K. Mehta, G. Kaur, R. Mutneja, K.K. Bhasin, J. Colloid Interface Sci. 338 (2009) 542-549.

Appendix C

Physicochemical studies of mixed surfactant microemulsions with isopropyl myristate as oil

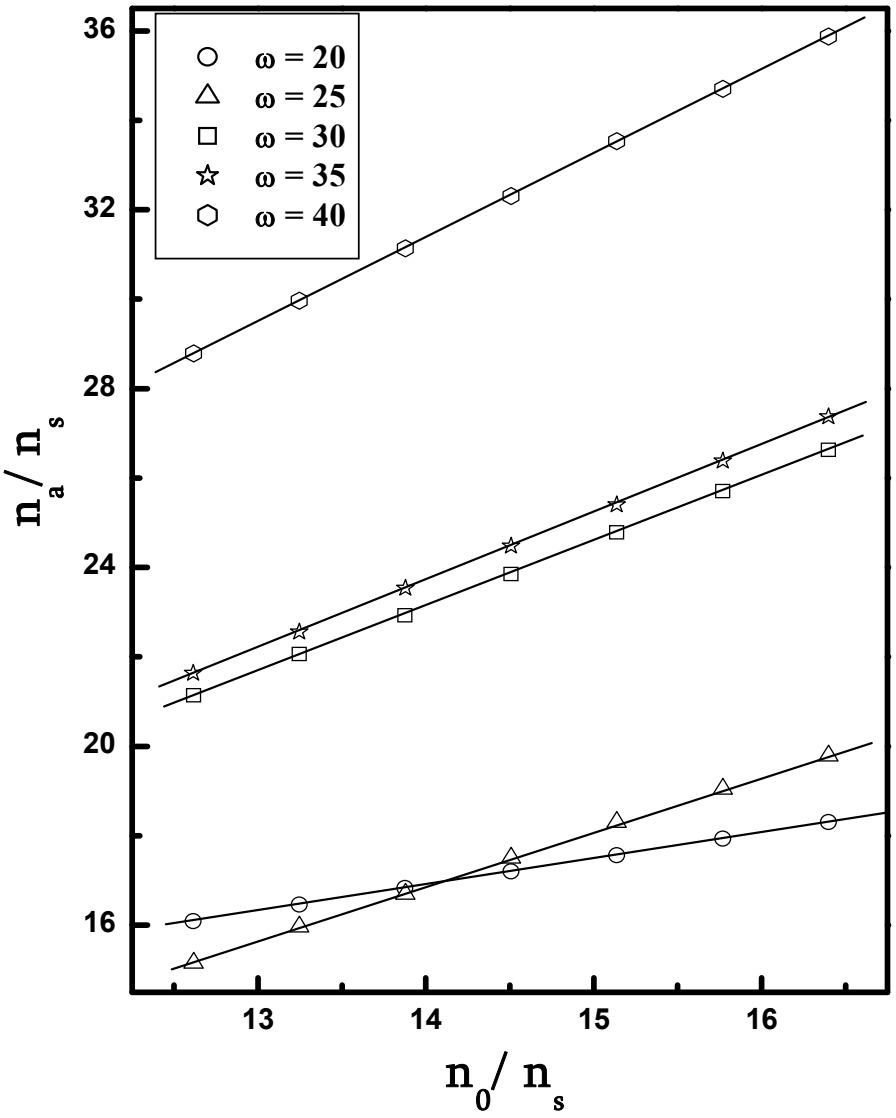

Fig. S1 Plots of n_a / n_s against n_0 / n_s according to Eq. (1) for w/o microemulsion systems comprising equimolar (1:1) mixed surfactant (SDS and Brij-35) (0.5 mmol) and IPM (14.0 mmol) stabilized by Pn with different ω (20→40) at constant temperature (303K).

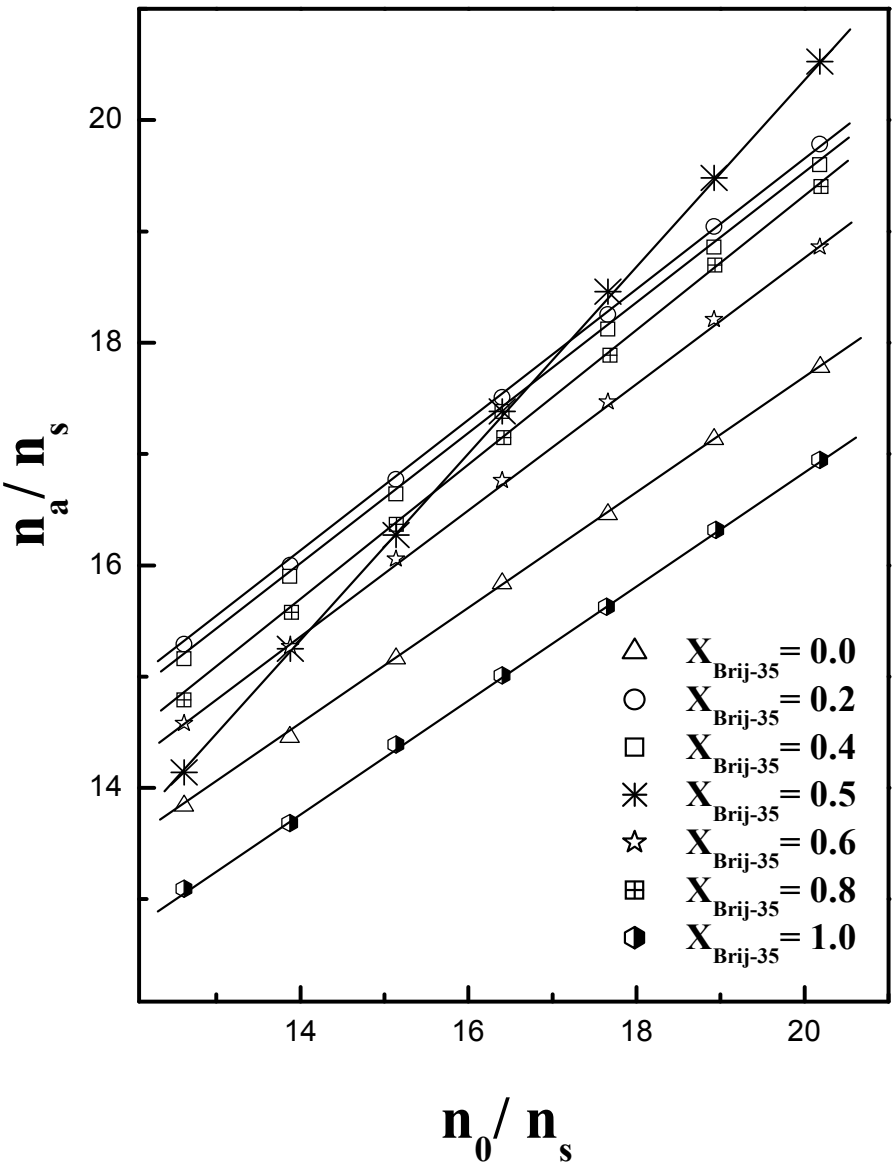

Fig. S2 Plot of n_a / n_s against n_0 / n_s according to Eq. (1) for w/o microemulsion systems comprising 0.5 mmol of mixed surfactant and 14.0 mmol of IPM oil stabilized by Pn with different ratios of mixed surfactant (SDS/Brij-35) at fixed water content (ω = 20) and constant temperature (303K).

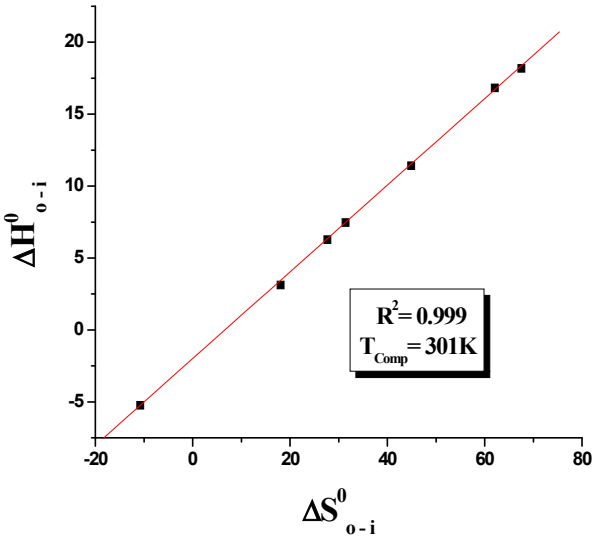

Fig. S3 Enthalpy-entropy compensation plots for the water/SDS/Brij-35/Pn/IPM (ω = 20) w/o microemulsion systems at 303K.

Table S1. Composition dependent specific heat capacity $[(\Delta C^0_P)_{o\rightarrow i}]$ for SDS/Brij-35/Pn/IPM/water w/o microemulsions systems

$X_{Brij-35}$	$-(\Delta C^0_P)_{o\rightarrow i}$ [kJ K^{-1} mol^{-1}]
0	0.18
0.2	0.25
0.4	0.19
0.5	0.04
0.6	0.99
0.8	0.95
1.0	0.62

Table S2. Compensation temperature (T_{comp}) from the plot of $\Delta H^0_{o\rightarrow i}$ against $\Delta S^0_{o\rightarrow i}$ for mixed surfactant microemulsion systems.

System	Experimental Temperature (K)	293	303	313	323
SDS/Brij-35/Pn/IPM/water	**Compensation Temperature (K)**	300	301	312	328
		[- 1.93][a]	[- 1.99]	[- 2.30]	[- 2.66]
		(0.998)[b]	(0.999)	(0.998)	(0.999)

[a] Values of intercept $[\Delta(H^0)^*_{o\rightarrow i}]$ of the plot, $\Delta H^0_{o\rightarrow i}$ against $\Delta S^0_{o\rightarrow i}$.
[b] Values of correlation of coefficients.

Appendix D

Formation, thermodynamic properties, microstructures and antimicrobial activity of mixed cationic/non-ionic surfactant microemulsions with isopropyl myristate as oil

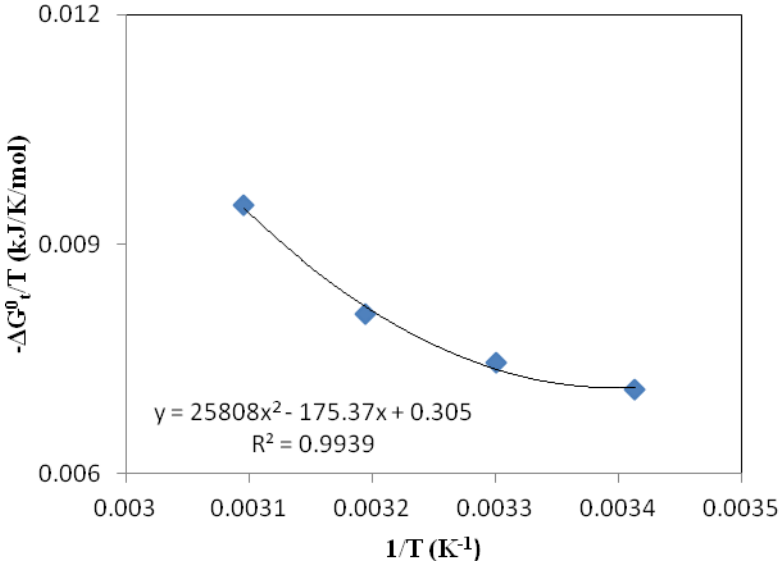

Fig. S1. Plot of (1/T) vs. (ΔG^0_t/T) for water/CTAB/1-pentanol/IPM system at fixed water content (ω = 20) using constant amount of mixed surfactant (0.5mmol) and oil (14.0 mmol).

1. Phase behavior of single and mixed surfactant microemulsions

Phase behavior actually determines the microstructure of the system [1]. Along with cosurfactant (Pn), CTAB/Brij-35 (mixed surfactants) has been found to favorably augment microemulsification (1ϕ region) of water and IPM. Phase diagram of pseudo-quaternary system, water/CTAB/Brij-35/Pn/IPM has been constructed in Gibbs triangle with the variation of Brij-35 ($X_{Brij-35}$ = 0.0, 0.2, 0.4, 0.5, 0.6, 0.8, 1.0) in a fixed amount of mixed surfactant (CTAB/Brij-35) and at a constant temperature of 303K (illustrative representation has been shown in Fig. 1 at $X_{Brij-35}$ = 0, 0.5 and 1.0, other figures are not exemplified here). The surfactant and cosurfactant ratio used was 1:2 (w/w). Each of the phase diagrams specifically indicates the presence of two different zones i.e., clear (microemulsion; 1ϕ region) and turbid (biphasic; 2ϕ region). Appearance of viscous and other phases along the [surfactant(s): cosurfactant/water]-oil axis have not been considered here for simplicity. Further, the size and location of above regions (1ϕ and 2ϕ) have been found to be dependent on the composition of mixed surfactant (CTAB and Brij-35) [2]. Similar result was also found in our previous report for water/SDS/Brij-35/Pn/IPM microemulsion [3]. However, it can be argued from the overall scenario that the characteristic of the phase diagrams is the appearances of considerable 1ϕ region i.e. clear solution along the amphiphile-oil axis which is actually oil continuous microemulsion with isolated and aggregated w/o dispersion.

2. Theoretical background of the dilution method

The w/o microemulsion consists of dispersion of water droplets in IPM continuum wherein the mixed surfactants were considered to populate at the oil/water interface in partial association with the cosurfactant (Pn), which remained distributed between the interface and the bulk oil. Thus, at a fixed [surfactant(s)], a critical concentration of Pn is required for the stabilization of the microemulsion. Addition of extra oil (IPM) extracts Pn from the interface to destabilize the system, which can be stabilized by the addition of extra cosurfactant(s) in the system. This is the fundamental basis of the dilution experiment. The following equations (detailed derivations are available in literatures [4, 5]) are helpful to rationalize the distribution and transfer process of Pn from the continuous oil phase to the interfacial region:

$$\frac{n_a}{n_s} = \frac{n_a^{\,w} + n_a^{\,i}}{n_s} + k\frac{n_o}{n_s} \tag{S1}$$

$$K_d = \frac{X_a^{\,i}}{X_a^{\,o}} = \frac{n_a^{\,i}/(n_a^{\,i} + n_s)}{n_a^{\,o}/(n_a^{\,o} + n_o)} = \frac{n_a^{\,i}\left(n_a^{o} + n_o\right)}{n_a^{\,o}(n_a^{\,i} + n_s)} \tag{S2}$$

where, $n_a, n_a^w, n_a^i, n_a^o, n_s$ denote the total number of moles of alkanol present, moles of alkanol in water, its number at the interface, in the oil phase and the total no of moles of surfactant respectively. The distribution constant of alkanol is represented by K_d where X_a^i and X_a^0 are the mole fraction of alkanol in the interfacial layer and in the oil.

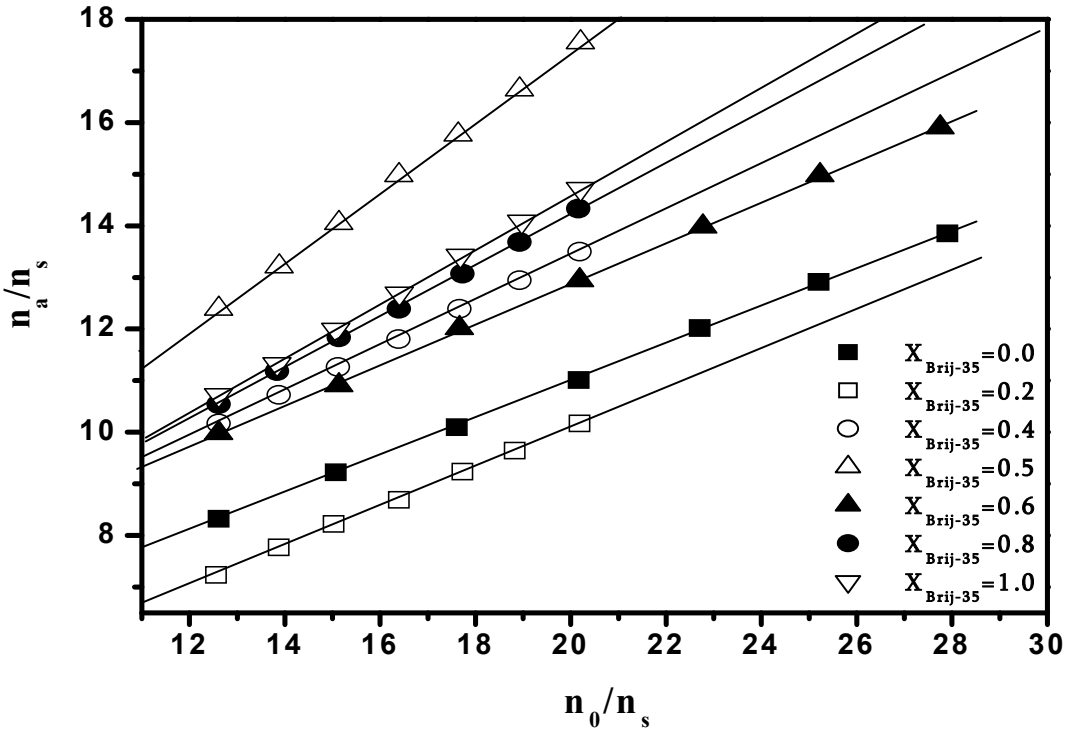

Fig. S2. Plots of n_a/n_s against n_0/n_s according to Eq. (S1) for w/o microemulsion systems comprising 0.5 mmol of mixed surfactant and 14.0 mmol of IPM oil stabilized by Pn with

different ratios of mixed surfactant(s) (CTAB and Brij-35) at fixed water content (ω = 20) and constant temperature (303K).

3. Effect of $X_{nonionic}$ and temperature on ΔH^0_t and ΔS^0_t of alkanol transfer process

Due to nonlinear dependence of (ΔG^0_t/T) on 1/T in terms of a two degree polynomial equation (Figs. are not illustrated), at each composition ($X_{Brij-35}$), four values of ΔH^0_t and ΔS^0_t at four temperatures have been evaluated, and are presented in Table 1. The profile of ΔH^0_t and ΔS^0_t with composition ($X_{Brij-35}$) and temperature (Figs. S3A and S3B) is not straightforward upon the addition of nonionic surfactant (Brij-35 with dodecyl hydrophobic tail) to the ionic surfactant (CTAB with cetyl hydrophobic tail) under various physicochemical conditions (as mentioned earlier).

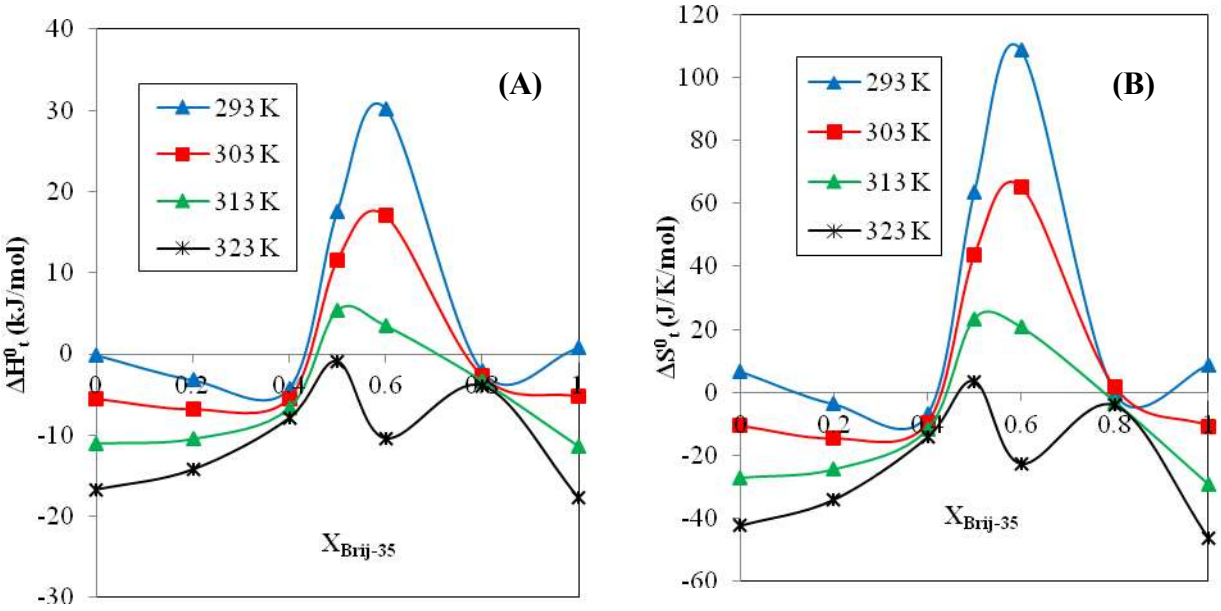

Fig. S3(A). Plot of ΔH^o_t against composition ($X_{Brij-35}$) for water/CTAB/Brij-35/Pn/IPM w/o microemulsion system comprising 0.5 mmol surfactant, 10 mmol water and 6.3 mmol IPM oil at different temperatures. **(B)** Plot of ΔS^o_t against composition ($X_{Brij-35}$) forthe same system under identical physicochemical conditions.

It is evident from Table 1 that, the overall transfer process is exothermic at all experimental temperatures with negative entropy change (except at 293 K) for single CTAB system. So, Pn causes release of heat during transfer process. Consequently, the negative entropy change was observed and might be due to organization of the interface and its surroundings. Therefore, the interfacial film composed of Pn and CTAB is to some extent more orderly. Such negative enthalpy and entropy changes were observed by De et al. [6] for water/DTAB/Pn/Hp microemulsion and Wang et al. [7, 8] for water or aqueous HCl/CTAC/octanol/diesel oil w/o microemulsion systems. For single Brij-35 stabilized system, the process is exothermic with release of heat at all experimental temperatures (except at 293 K) with negative entropy change (order) in IPM. Negative values of ΔS^0_t suggest that the entropy as well as enthalpy are involved in the transfer process at the corresponding composition [9]. Such negative enthalpy and entropy changes were observed by Mehta et al. [10] for water/Brij-96/Pn/ethyl oleate (EO) system.

At compositions in between these two extremes (i.e. at $X_{Brij-35}$ = 0.2, 0.4 and 0.8), both ΔH^0_t and ΔS^0_t values are negative whereas at $X_{Brij-35}$ = 0.5 and 0.6, the values of ΔH^0_t and ΔS^0_t are positive (except for few compositions at 323 K). An interesting feature reveals from the Table 1 and Figs. S3A and S3B that both ΔH^0_t and ΔS^0_t values decrease with increase in temperature at all mixed compositions. In other words, the transfer process ($Pn_{oil} \rightarrow Pn_{int}$) changes from endothermic to exothermic (at $X_{Brij-35}$ = 0.5 and 0.6) or less exothermic to more exothermic (at $X_{Brij-35}$ = 0.2, 0.4 and 0.8) with increase in temperature. A plausible explanation for exothermicity or endothermicity-derived process may be as follows. The positive contribution towards ΔH^0_tcan be the energy required to release the structural water from the hydration layer around the hydrophilic domain. An additional contribution arises from the liberation of water molecules from the hydrophilic moiety of the surfactants. The negative contribution towards ΔH^0_t isidentified with the transfer of the surfactant tail from water to liquid hydrocarbon state in the interfacial layer and restoring the hydrogen bonding structure of the water around the surfactant head group. With increase in temperature, the degree of hydrogen bonding around the surfactant molecules decreases, and therefore, the energy required tobreak it diminishes i.e., ΔH^0_tdecreases with temperature [11].It is apparent that different phenomena associated with the transfer process, viz., changing aggregation number, solvation-desolvation of nonionic surfactants, electrostatic and steric interaction between hydrophilic head group of ionic and nonionic surfactants, steric and other nonspecific processes contribute their shares to the ΔH^0_t and ΔS^0_t [12]. Hence, it can be inferred that the overall mixed surfactant microemulsion forming systems can end up with both absorption or release of heat and with ordered or disordered state, depending on the content of nonionic surfactant ($X_{nonionic}$) in mixed cationic/nonionic system and thermal condition.

However, a comparison of the thermodynamic properties of the present system (cationic-nonionic) and previously reported (anionic-nonionic), water/SDS/Brij-35/Pn/IPM microemulsion system [3] is presented as follows. It can be seen that ΔH^0_t and ΔS^0_t are exothermic with overall ordered respectively, at compositions ($X_{Brij-35}$ = 0→0.4 and 0.8→1.0) for the former system. However, ΔH^0_t and ΔS^0_t were endothermic and overall disordered respectively, at all compositions ($X_{Brij-35}$ = 0→0.8) for the formation of later system. The plausible explanations are as follows: It was reported earlier that the polar head groups of anionic and cationic surfactants are located in a different region of the polyoxyethylene mantle of the anionic/nonionic or cationic/nonionic mixed systems, respectively[13]. The location or spatial arrangement of the surfactants with different charge types and equal or unequal hydrocarbon chains at the interface is attributed to the type and nature of polar head groups involved therein. An explanation at a molecular level of overall thermodynamic behaviors of these mixed microemulsion systems can be presented according to view points of Dominguez [14] from computer simulation study. According to this report, the structure of the interfacial water molecules is different around the anionic (herein, SDS) and the cationic (herein, CTAB) molecules, as well as the average dipole orientation at the interface in each mixture also differs. Even more, close to the nonionic head group (herein, POE chains of Brij-35), the orientation of water is also different in these mixtures. The respective counter ion distribution in each mixture might also be different. Therefore, the properties of the nonionic surfactant are influenced not only by the charge distribution of the ionic surfactants but also by the interaction between water and the counter ions.For instance, the position of the nonionic surfactant molecules and their orientations are not the same at the interface as that of the anionic or the cationic surfactant molecules. Further, the anionic surfactant molecules penetrate more into water for the anionic-nonionic mixtures, and subsequently, water is closer to the anionic head groups than to the nonionic head groups. Moreover, the water hydrogen next to the anionic surfactant molecules point towards the central group, whereas hydrogen next to the nonionic surfactant molecules seems to be point away from that group. On the other hand, the nonionic surfactant penetrates slightly deeper in the water region for the cationic-nonionic surfactant mixtures. As a result, water near to the surfactants is slightly closer to the cationic than to the nonionic head groups. In this case water oxygen is pointing towards the positive head

group. It can be inferred that the endothermic contribution for the anionic-nonionic mixtures comes from the liberation of water molecules from the hydrophilic moiety of both anionic and nonionic surfactants, whereas the exothermic contribution comes from restoring the hydrogen bonding structure of the water around the cationic and nonionicsurfactant head groups in the cationic-nonionic mixtures [11]. Apart from that, because of the presence of unequal hydrocarbon tails of CTAB (C_{16}) and Brij-35 (C_{12}) in the mixed surfactant film, the excess hydrocarbon tails might have more freedom to disrupt the molecular packing through conformational disorder, increased tail motion, or other factors [15]. This disruption in the molecular packing may contribute to the thermodynamic parameters (ΔH^0_t and ΔS^0_t) of Pn transfer process.

Effect of $X_{nonionic}$ on $(\Delta C^0_p)_t$ of alkanol transfer process

Since ΔH^0_t became a function of temperature, the $(\Delta C^0_p)_t$ values have also been obtained at all compositions from the slope of the plots of ΔH^0_t vs. T (Figures are not exemplified) according to Eq. (S8). All these values are negative (presented in Table S1) and agree well with those reported by Mitra et al. [16] for water/CTAB or its analogues with modified head group/Hx/i-Oc, Bardhan et al. [3] for water/SDS/Pn/IPM and Kundu et al. [4, 5] for water/CPC or SDS/Brij-58 or Brij-78/Pn/Hp or Dc microemulsion systems, respectively. Such negative values are usually observed for the self-association of amphiphiles and can be attributed to the removal of large areas of non-polar surface from contact with water on theformation of reverse micelles [17].

Correlation between ΔH^0_t and ΔS^0_t

In kinetics and equilibrium studies, an extra thermodynamic linear correlation between ΔH^0_t and ΔS^0_t for the involved process is often reported, called the enthalpy-entropy compensation effect, and such a phenomenon has been observed to be valid also for micelle and microemulsion forming systems [4, 5, 10, 18, 19]. In general, the compensation effect can be described by a liner relationship in the form [20]:

$$\Delta H^0_t = T_{comp}.\Delta S^0_t + \Delta(H^0)^*_t \qquad \text{(S3)}$$

where, T_{comp}, is the slope of the compensation plot and $\Delta(H^0)^*_t$, the intrinsic enthalpy change of Pn transfer process is the intercept. According to the working scheme of Lumry and Rajender[20] for a compensation phenomenon, the micellization or microemulsification can be described as consisting of two-part processes: (a) the "desolvation" part, i.e., the dehydration of the hydrocarbon tail or polar head of surfactant molecules, and (b) the "chemical" part, i.e., aggregation of the hydrocarbon tails or polar headgroup of surfactant molecules to form micelle or reverse micelle. T_{comp} can be interpreted as a characteristic of solute-solute and solute-solvent interactions, i.e., proposed as a measure of the "desolvation" part. $\Delta(H^0)^*_t$ characterizes the solute-solute interaction, i.e., considered as an index of the "chemical" part. The thermodynamic results herein collected were tested for this correlation and illustrated as representative plot for CTAB/Brij-35/Pn/IPM/water at 293K [Fig. S4]. A good linear correlation was observed at the temperature of measurement (regression coefficients are 0.9995) i.e. mutual compensation temperature of 299.3 K, which was higher by ~6K than the temperature of measurement (293K). T_{comp} and $\Delta(H^0)^*_t$, obtained at different experimental temperatures (293, 303, 313 and 323K) for these systems are presented in Table S2. T_{comp} temperatures are slightly deviated from the experimental temperatures. Such a deviation is quite common in literature [4, 5, 18]. In our previous report [18], the discrepancy between experimental and compensation temperatures were elaborately discussed. Further, it reveals from Table S2 that the values of $\Delta(H^0)^*_t$ lie in the range of -2.01 kJ/mol to - 2.57 kJ/mol. $\Delta(H^0)^*_t$ increase with increase in experimental temperature for CTAB/Brij-35 system in IPM. There exists an equilibrium between (free water in bulk solvent + free surfactant molecules with associated water and solvent molecules) and (surfactants with associated water and solvent molecules in the reverse micelles + released solvent molecules). Increasing experimental temperature weakens molecular interactions which results in shifting the surfactant monomer-reverse micelle equilibrium toward the monomer which affects aggregation of surfactant molecules as well as $\Delta(H^0)^*_t$ [21]. Similar observation was also reported by Kundu et al. [4, 5] and Bardhan et al. [3].

The aforesaid analysis of the thermodynamics of the studied transfer process can be summarized as follows: ΔG^0_t consists of a number of factors which may account respectively for the transfer of surfactants (CTAB and Brij-35) and Pn tails from oil to the interfacial film, the deformation of the tails to satisfy packing constraints, the free energy of formation of the oil/water interface, the steric and ionic interactions among the head groups of CTAB as well as interaction arising out of dissimilar head groups and hydrocarbon chain length of both CTAB and Brij-35, the free energy of mixing of surfactants, Pn, and oil (IPM) in the film region [22] and free energy due to formation of hydrated nonionic surfactant (Brij-35) results in formation of different states of water in the pool[23]. As a result of these possible contributions towards ΔG^0_t at different temperatures, heat involving processes and consequently conformational entropy due to packing restrictions of the hydrocarbon chains, and entropy of mixing the two surfactants in the aggregates make the thermodynamics more complex. Such a comprehensive analysis on the formation and stability of w/o mixed surfactant microemulsions in IPM based on "Bowcott and Schulman model" [24] from the view point of thermodynamics, is scarcely reported in literature. Further studies along these series of measurements to shed more quantitative description of these thermodynamic quantities are warranted.

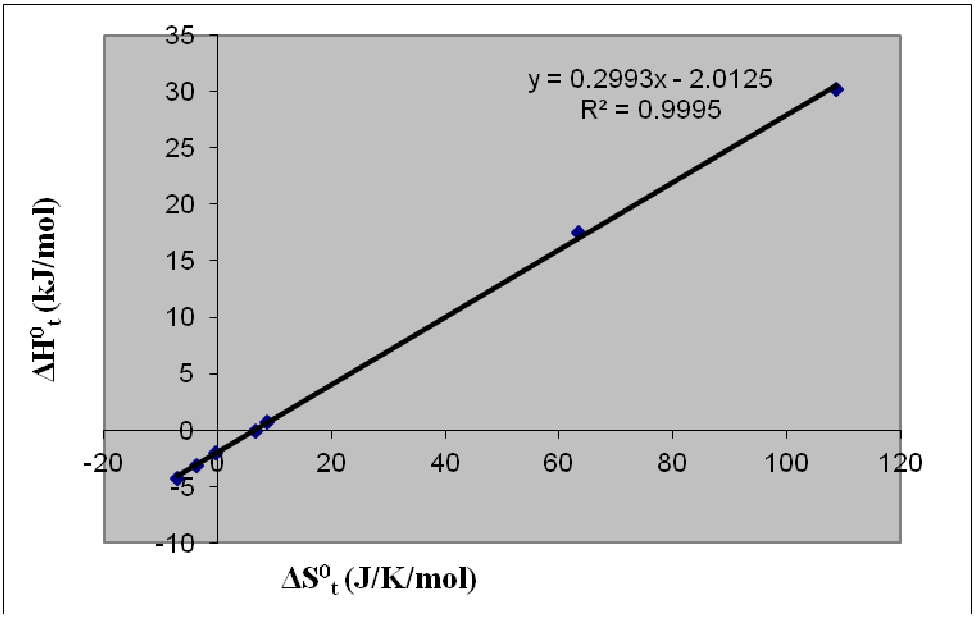

Fig. S4. Enthalpy-entropy compensation plot for water/CTAB/Brij-35/Pn/IPM w/o microemulsion systems at 293K.

Table S1. Composition dependent specific heat capacity [$(\Delta C^0_P)_t$] from the plot of ΔH^0_t vs. T for CTAB/Brij-35/Pn/IPM/water w/o microemulsions systems.

$X_{Brij-35}$	$-(\Delta C^0_P)_t$ (kJ K^{-1} mol^{-1})
0	0.55
0.2	0.37
0.4	0.12
0.5	0.63
0.6	1.35
0.8	0.06
1.0	0.62

Table S2. Compensation temperature (T_{comp}) from the plot of ΔH^0_t against ΔS^0_t for mixed surfactant microemulsion systems.

System	**Experimental Temperature (K)**	**293**	**303**	**313**	**323**
CTAB/Brij-35/Pn/IPM/water	**Compensation Temperature (K)**	299.30 [- 2.01][a] (0.9995)[b]	302.70 [- 2.21] (0.9987)	315.70 [- 2.53] (0.9969)	336.60 [- 2.57] (0.9968)

[a] Values of intercept [$\Delta(H^0)^*_t$] of the plot, ΔH^0_t against ΔS^0_t; [b] Values of correlation of coefficients.

4. Transport property: Effect of ω and $X_{nonionic}$ on conductivity of mixed surfactant microemulsion

In the present report, the dependence of electrical conductivity (σ) on water content (ω) as a function of composition ($X_{Brij-35}$ = 0.0→1.0) in water/CTAB/Brij-35/Pn/IPM system has been systematically investigated at a fixed surfactant concentration (0.3 mol dm^{-3}) and temperature (303K) and the results are presented in Fig. S5.It can be observed from Fig. S5 that the single CTAB microemulsion system (at $X_{Brij-35}$ = 0.0) is low conducting and does not exhibit any significant increase in conductivity with increase in ω. Similar observation was also reported earlier for water/AOT/IPM [25] and water/SDS/Pn/IPM microemulsion systems [3]. However, the addition of nonionic surfactant (herein, Brij-35) to the water/CTAB/Pn/IPM system with fixed total surfactant concentration (as mentioned above), a dramatic increase in conductivity has been observed as a function of ω up to equimolar composition ($X_{Brij-35}$ = 0.2→0.5), beyond which

($X_{Brij-35}$ = 0.6→1.0) results in a small decrease in conductivity with increasing ω. An in-depth analysis of the results reveals that conductivity increases slowly with ω and after that a sharp increase is observed at a certain ω for $X_{Brij-35}$ = 0.2, 0.4 and 0.5 blends (Fig. S5). The critical value for sharp linear enhancement in conductivity (σ) with the addition of water is considered as percolation threshold point [10]. The critical value of ω for $X_{Brij-35}$ = 0.2, 0.4 and 0.5 has been found to be ω ≤ 27.57, ω ≤ 34.83 and ω ≤ 39.05, respectively. Actually, percolation of conductance extracts information about the nature of interaction among the droplets in microemulsions. If the droplets are of non-interacting hard sphere type, no significant increase in conductance occurs with increasing water content. When interfaceof the droplets is fluid enough to coalesce during these collisions followed by material exchange and fusion, a sharp rise in conductance is evidenced [26]. Percolation of conductance signifies the increase in droplet size, attractive interaction among droplets and exchange rate of materials between the droplets with the addition of water [27]. Similar observation was also evidenced in our previous report for water/SDS/Brij-35/Pn/IPM microemulsion systems [3]. However, from acomparative study it can be observed that threshold point of percolation occur much earlier in water/SDS/Brij-35/Pn/IPM microemulsion systems compared to the present systems at comparable physicochemical conditions. It may be due to the basic differences in chemical structure, hydrophobic chain length, charge type, and location of the ionic charge vis-à-vis their exposure to experimental medium between CTAB and SDS (as mentioned in Sec. 3.2.2 of main text) [28]. As a result, hydrated charge carriers for SDS derived systems are randomly redistributed and formed separately charged droplets to induce percolation phenomena earlier compared to CTAB derived systems.

The addition of Brij-35to single CTAB based microemulsion, critical packing parameter (CPP) [25, 29] of mixed microemulsionsystems decreases and thereby leads to increase in the droplet radius with increase in $X_{Brij-35}$ [27]. As a result, the attractive interaction between the aggregates increases, forming cluster with water channels, through which the charge carriers can move efficiently, resulting in percolation phenomena. Further, it can be observed from Fig. S5 that threshold point of percolation increases with increase in $X_{Brij-35}$ up to 0.5 at a fixed temperature and thereafter no such phenomenon is evidenced. It can be argued as follows. After the addition of water to the pseudo-ternary system (at $X_{Brij-35}$ = 0.2→0.8), polar head groups of both CTAB [$N(CH_3)_3^+$] and Brij-35 (POE) surfactants have a tendency to form strong hydrogen bond with water [30]. In addition,a strong ion-dipole interaction between trimethylammonium group [$N(CH_3)_3^+$] in CTAB and EO groups in Brij-35 exists within the water pool. It is quite likely that the origin of these interactions comes from the hydrogen bond formation between the trimethylammonium polar head groups and dehydrated EO chains in the mixed corona, makes the corona more compact [31]. All these attractive interactions lead to the rigidification of the mixed surfactant monolayer [32, 33] and thereby, percolation threshold increases from $X_{Brij-35}$ = 0.2 to 0.5 (that is equimolar composition). Beyond which, (that is, $X_{Brij-35}$ = 0.6→1.0), increase in droplet size (dealt in Sec. 3.4 of main text which deals with DLS measurement) results in decrease in mobility of the charged droplets. This favors the formation of an electrical double layer, which is responsible for increase in repulsive interaction between the droplets and lowers the conductivity [34]. Similar studies on percolation of conductance phenomenon were also reported for single nonionic (Brij-96) or ionic (CTAB or SDS or OTAB or AOT) surfactant derived microemulsions in presence of cosurfactant [10, 35, 36].

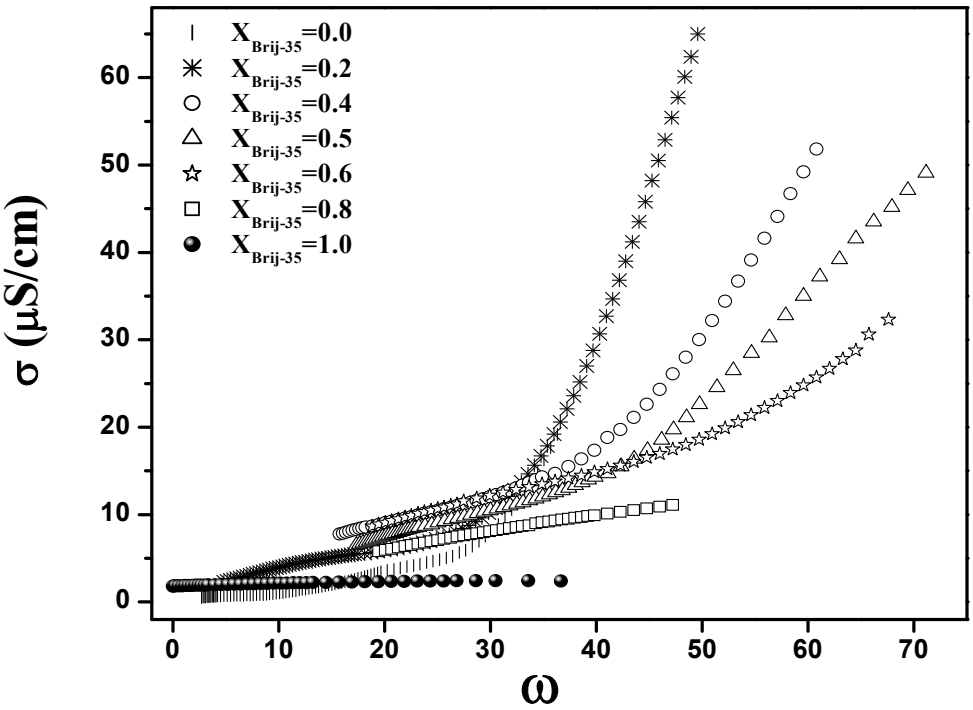

Fig. S5. Conductivity (σ) against ω profile with the variation of $X_{Brij-35}$ (= 0.0→1.0) for water/CTAB/Brij-35/Pn/IPM w/o microemulsion systems at fixed surfactant concentration (0.3 mol. dm^{-3}) and constant temperature (303K).

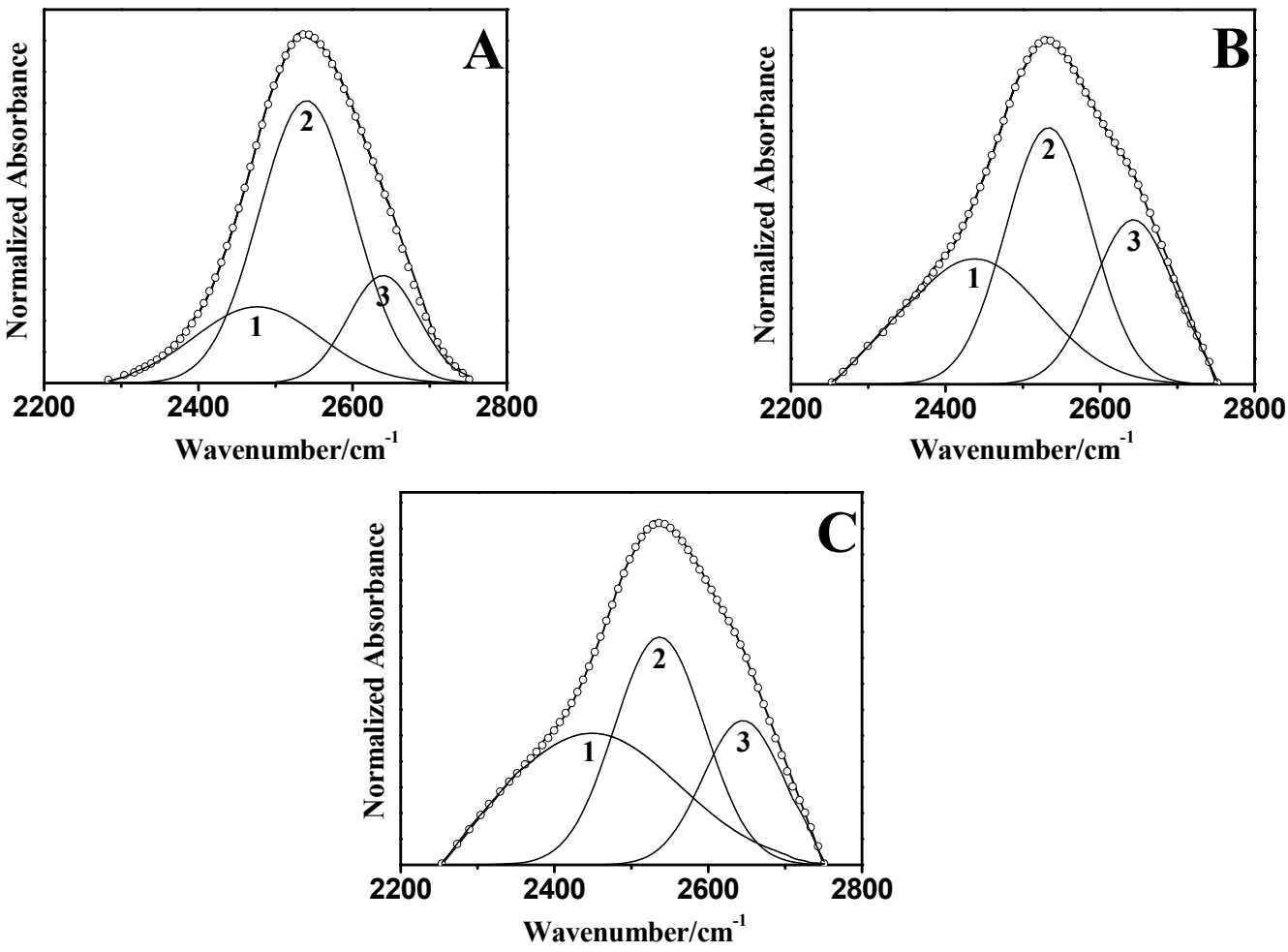

Fig. S6. Representative FTIR spectra of O-D band of HOD solubilized in mixed surfactant (CTAB/Brij-35) w/o microemulsion systems at fixed ω (= 20) and surfactant-cosurfactant mass ratio (1:2) [A : $X_{Brij\text{-}35}$ = 0.0; B: $X_{Brij\text{-}35}$ = 0.5; C: $X_{Brij\text{-}35}$ = 1.0 [Specification: Experimental spectra, overall fitted curve (open circle) and deconvoluted curves (*1: free water; 2: bound water; 3: trapped water*)].

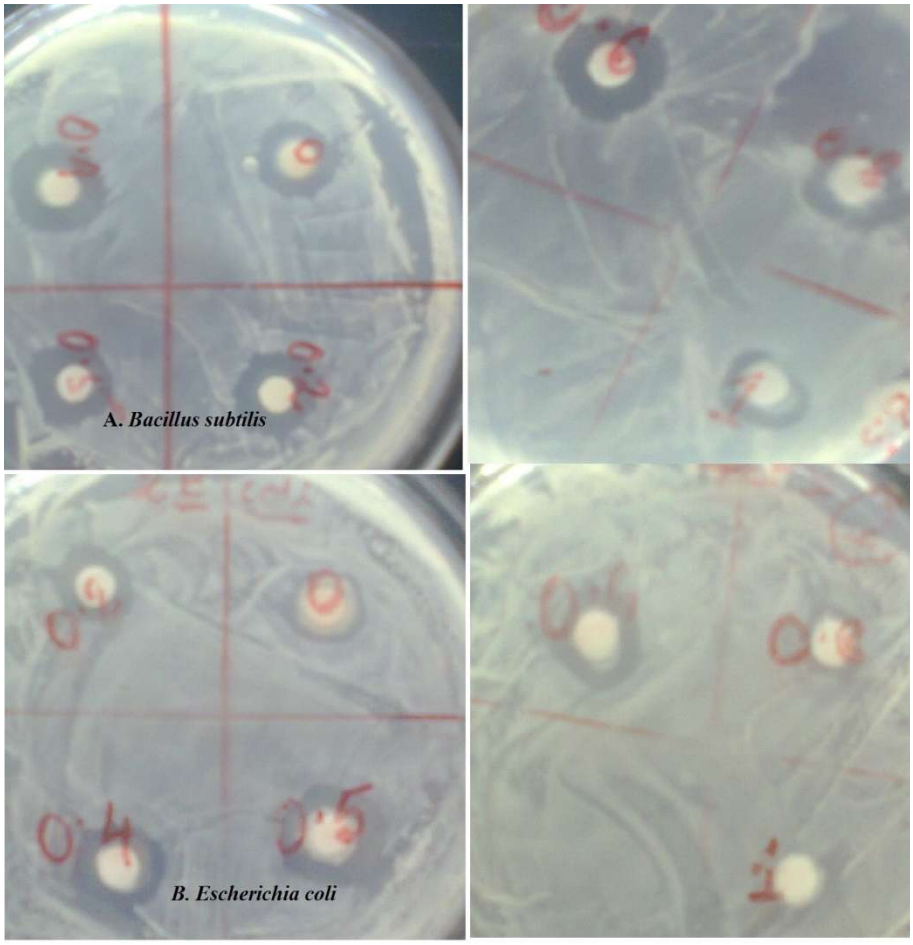

Fig. S7. Representative images in agar plates showing the inhibition zones produced by w/o mixed surfactant microemulsions with the variation of $X_{Brij\text{-}35}$ (= 0.0, 0.2, 0.4, 0.5, 0.6, 0.8 and 1.0) at fixed water content(ω = 20) and temperature (303K) against *B. subtilis* and *E. coli.*

Table S3. Diameters of inhibition zones (diz) produced by the constituents of the water/CTAB/Brij-35/Pn/IPM microemulsions at temperature (303K) against *B. subtilis* and *E. coli.*

	Diameters of inhibition zones against bacterial strains in mm	
***[CTAB] (mmol)*[a]**	*B. subtilis* (gram positive)	*E. coli* (gram negative)
0.50[b]	12.0	10.0
0.40	11.0	9.0
0.30	10.0	8.0
0.25	9.0	8.0
0.20	9.0	7.5
0.10	8.0	7.0
0.0	-	-
Brij-35[c]	0.7	0.6
Pn[d]	0.6	0.5
IPM	—	—

[a] CTAB at the same concentration in water as used for the formulation of w/o mixed surfactant microemulsions with the variation of $X_{Brij\text{-}35}$ (= 0.0→1.0). [b] Best inhibitor for *B. subtilis* and *E. coli* respectively. [c] Brij-35 in water at highest solubilization limit (= 0.03 M at 303K). [d] Pn at the same concentration in IPM due to its negligible water solubility.

Table S4. Diameters of inhibition zones (diz) produced by water/CTAB/Brij-35/Pn/IPM microemulsions with the variation of $X_{Brij\text{-}35}$ (= 0.0→1.0) at fixed water content (ω = 20) and temperature (303K) against *B. subtilis* and *E. coli.* respectively.

$X_{Brij\text{-}35}$	**Diameters of inhibition zones against bacterial strains in mm (Efficacy of the microemulsion formulation)**	
	B. subtilis (gram positive)	*E. coli* (gram negative)
0.0 ([CTAB] = 0.5, [Brij-35] = 0)[a]	13.0 (1.08)[b]	9.0 (0.90)[b]
0.2 ([CTAB] = 0.4, [Brij-35] = 0.1)	14.0 (1.17)	10.0 (1.00)
0.4([CTAB] = 0.3, [Brij-35] = 0.2)	18.0 (1.50)	15.0 (1.50)
0.5 ([CTAB] = 0.25, [Brij-35] = 0.25)	15.0 (1.25)	12.0 (1.20)
0.6 ([CTAB] = 0.2, [Brij-35] = 0.3)	17.0 (1.42)	14.0 (1.40)
0.8 ([CTAB] = 0.1, [Brij-35] = 0.4)	15.6 (1.30)	13.0 (1.30)
1.0 ([CTAB] = 0, [Brij-35] = 0.5)	11.0 (0.92)	10.0 (1.00)

[a] [CTAB] and [Brij-35] are expressed in mmol. [b] Parenthetic values represent the comparative efficiency of the microemulsion formulations.

References

[1] A. Yaghmur, A. Aserin, N. Garti, Colloids Surf. A 209 (2002) 71.
[2] M. Kahlweit, B. Faulhaber, G. Busse, Langmuir10 (1994) 2528.
[3] S. Bardhan, K. Kundu, S.K. Saha, B.K. Paul, J. Colloid Interface Sci. 402 (2013) 180.
[4] K. Kundu, G. Guin, B.K. Paul, J. Colloid Interface Sci. 385 (2012) 96.
[5] K. Kundu, B.K. Paul, Colloid Polym. Sci. 291 (2013) 613.
[6] M. De, S.C. Bhattacharya, A.K. Panda, S.P. Moulik, J. Disp. Sci. Technol. 30 (2009) 1262.
[7] F. Wang, B. Fang, Z. Zhang, S. Zhang, Y. Chen, Fuel 87 (2008) 2518.
[8] F. Wang, B. Fang, Z. Zhang, L. Qiao, Y. Chen, J. Chem. Eng. Data 53 (2008) 1256.
[9] S. Ghosh, A.D. Burman, G.C. De, A.R. Das, J. Phys. Chem. B 115 (2012) 11098.
[10] S.K. Mehta, G. Kaur, R. Mutneja, K.K. Bhasin, J. Colloid Interface Sci. 338 (2009) 542.
[11] J. Łuczak, C. Jungnickel, M. Joskowska, J. Thöming, J. Hupka, J. Colloid Interface Sci. 336 (2009) 111.
[12] G.B. Ray, I. Chakraborty, S. Ghosh, S.P. Moulik, J. Colloid Interface Sci. 307 (2007) 543.
[13] P. Baglioni, L. Dei, L. Kevan, E.R-. Minten, ACS Symp. Series, Washington DC, 1992, pp. 180-193.
[14] H. Dominguez, J. Colloid Interface Sci. 274 (2004) 665.
[15] S.Y. Shiao, V. Chhabra, A. Patist, M.L. Free, P.D.T. Huibers, A. Gregory, S. Patel, D.O. Shah, Adv. Colloid. Interface Sci. 74 (1998) 1.
[16] D. Mitra, I. Chakraborty, S.C. Bhattacharya, S.P. Moulik, S. Roy, D. Das, P.K. Das, J. Phys. Chem. B 110 (2006) 11314.
[17] S.K. Mehta, S. Chaudhary, K.K. Bhasin, J. Colloid Interface Sci. 321 (2008) 426.
[18] R.K. Mitra, B.K. Paul, S.P. Moulik, J. Colloid Interface Sci. 300 (2006) 755.
[19] G. Liu, D. Gu, H. Liu, W.Ding, Z. Li,J. Colloid Interface Sci. 358 (2011) 521.
[20] R. Lumry, S. Rajender, Biopolymers 9 (1970) 1125.
[21] D.M. Zhu, K.I. Feng, Z.A. Schelly, J. Phys. Chem. 96 (1992) 2382.
[22] R. Nagarajan, E. Ruckenstein, Langmuir 16 (2000) 6400.
[23] N.E. Levinger, L.A. Swafford, Ann. Rev. Phys. Chem. 60 (2009) 385.
[24]J.E. Bowcott, J.H. Schulmann, Z. Electrochem. 59 (1955) 283.
[25] R.K. Mitra, B.K. Paul, Colloids Surf. A 252 (2005) 243.
[26] B.K. Paul, R.K. Mitra, S.P. Moulik, In: P. Somsundaran, (Ed.) Encyclopedia of Surf. Colloid Sci.; Taylor and Francis: New York, 2006; pp 3927-3956.
[27] B.K. Paul, R.K. Mitra, J. Colloid Interface Sci. 288 (2005) 261.
[28] A. Bera, K. Ojjha, T. Kumar, A. Mandal, Colloids Surf. A 404 (2012) 70.
[29] K. Kundu, B.K. Paul, Colloids Surf. A 433 (2013) 154.
[30]T.P. Goloub, R.J. Pugh, J. Colloid Interface Sci. 291 (2005) 256.
[31] T.P. Goloub, A.D. Keizer, Langmuir 20 (2004) 9506.
[32] W. Meier, J. Phys. Chem. B 101 (1997) 919.
[33] Y. Gao, N. Li, L. Zheng, X. Bai, L. Yu, X. Zhao, J. Zhang, M. Zhao, Z. Li, J. Phys. Chem. B 111 (2007) 2506.
[34] N. Kallay, A. Chittofrati, J. Phys. Chem. 94 (1990) 4755.
[35] S. Paul, S. Bisal, S.P. Moulik, J. Phys. Chem. 96 (1992) 896.
[36] K. Maiti, I. Chakraborty, S.C. Bhattacharya, A.K. Panda, S.P. Moulik, J. Phys. Chem. B 111 (2007) 14175.

Appendix E

Physicochemical investigation of mixed surfactant microemulsion: Water solubilization, thermodynamic properties, microstructure and dynamics

1. A. Dilution method with spectrophotometric measurements

Fixed amounts of mixed surfactants (Brij-58 and CTAB) at different proportions, water and oil (Hp and Dc) were mixed in a dry test tube and kept in a thermostated water bath (accuracy, ± 0.1 K) at fixed temperature. Cosurfactant (Pn) was gradually added in small intervals into it from a Hamilton micro-syringe (Hamilton, USA) with constant stirring until a clear single-phase solution appeared and the critical volume of Pn was noted. After that, a calculated small amount of oil was then added into it and the formulation reverted back to the biphasic form. This biphasic mixture was again titrated with Pn until the appearance of single-phase with quantification by spectrophotometer. This procedure was repeated noting the required volume of Pn necessary at each step for obtaining a clear and stable w/o microemulsion. The entire procedure was monitored at five different temperatures viz. 303, 308, 313, 318 and 323K. The change in sample turbidity to clear solution by alkanol (Pn) addition has been measured by using spectrophotometric technique [1]. To a turbid solution comprising a blend of Brij-58 and CTAB at different composition and water in a given solvent (Hp or Dc) at 303 K, small aliquots of Pn was added. The point of single-phase microemulsion formation was evidenced by a total loss of sample turbidity, checked by the sample absorbance measured at 320 nm [1]. The sharp decrease in absorbance observed in the sample titration with alkanol (Pn) allows precise determination of the amount cosurfactant needed to stabilize the microemulsion. The absorbance measurements were carried out at 320 nm in JASCO (V-530) UV-spectrophotometer employing thermostated cell. The amount of mixed surfactant(s) and oil(s) was taken as 0.5 mmol and 14.0 mmol, respectively for each system.

B. Basic equations for evaluation of interfacial composition and energeticparameters for transfer process:

The interfacial composition and energetic of the self-assembly process of amphiphiles (mixed surfactants and alkanol) in (w/o) microemulsion was evaluated with the following relations which actually hold by the mass balance consideration in the dilution experiment [1-4]

$$\frac{n_a{}^t}{n_s} = \frac{n_a{}^w + n_a{}^i}{n_s} + k\frac{n_o}{n_s} \tag{S1}$$

In our experiment, negligible water solubility of Pn leads to $n_a{}^w \approx 0$ [3, 4].Thus, above equation becomes,

$$\frac{n_a}{n_s} = \frac{n_a^i}{n_s} + k_o\frac{n_o}{n_s} \tag{S2}$$

$$K_d = \frac{X_a{}^i}{X_a{}^o} = \frac{n_a{}^i/(n_a{}^i + n_s)}{n_a{}^o/(n_a{}^o + n_o)} = \frac{n_a{}^i\left(n_a^o + n_o\right)}{n_a{}^o(n_a{}^i + n_s)} \tag{S3}$$

$$\Delta G_t^0 = -RT\ln K_d \tag{S4}$$

where, $n_a^t, n_a^w, n_a^i, n_a^o, n_s$ denote the total number of moles of alkanol present, moles of alkanol in water, its number at the interface, in the oil phase and the total no of moles of surfactant, respectively. The distribution constant of alkanol is represented by K_d where X_a^i and X_a^0 are

the mole fraction of alkanol in the interfacial layer and in the oil. ΔG^0_t represents standard Gibbs free energy change of transfer of alkanol from oil to the interface.
ΔH^0_t (standard enthalpy change of transfer of alkanol from oil to the interface) can be evaluated by the van't Hoff equation. Thus,

$$[\partial(\Delta G^0_t/T)/\partial(1/T)]_p = \Delta H^0_t \quad \text{(S5)}$$

Since the dependency of $(\Delta G^0_t/T)$ on (1/T) are nonlinear for all these systems [plot of $(\Delta G^0_t/T)$ vs. (1/T) water/Brij-58/CTAB/Pn/Hp system at fixed Brij-58: CTAB (= 3:2, w/w) and water content (2.75×10^{-2}mol) (Fig. S2), same plots for other systems have not been exemplified], a two-degree polynomial equation of following form is used.

$$\left(\frac{\Delta G^0_t}{T}\right) = A + B_1\left(\frac{1}{T}\right) + B_2\left(\frac{1}{T}\right)^2 \quad \text{(S6)}$$

The differential form of the relation helps to evaluate ΔH^0_t. Thus,

$$\frac{\partial\left(\Delta G^0_t/T\right)}{\partial\left(1/T\right)} = B_1 + 2B_2\left(\frac{1}{T}\right) = \Delta H^0_t \quad \text{(S7)}$$

where, A, B_1 and B_2 are the polynomial coefficients.
Then the Gibbs-Helmholtz equation is used to evaluate ΔS^0_t (standard entropy change of transfer of alkanol from oil to the interface).

$$\Delta S^0_t = \frac{\Delta H^0_t - \Delta G^0_t}{T} \quad \text{(S8)}$$

The standard state herein considered is the hypothetical ideal state of the unit mole fraction.

2. Phase behavior

For w/o microemulsion system consisting of mixed surfactants, it is important to have an idea of the phase diagram of the system. The pseudo-ternary phase diagram of Brij-58-based quaternary system showsthat with the addition of CTAB to the chosen surfactant-cosurfactant (S/CS = 1: 2, w/w) and oil (Hp or Dc) mixtures, there is a continuous enhancement in single phase microemulsion (1ϕ) zone, as revealed from representative phase diagram and plot of 1ϕ (%) versus mixed surfactant composition (Fig. S1). During the determination of single phase (1ϕ) clear microemulsion region, viscous and biphasic regions were appeared along the water-oil axis, which have not been shown in the Fig. S1 for the sake of simplicity. Phase behavior actually determines the microstructure of the system. The microstructure of the microemulsions depends on the spontaneous film curvature and the elasticity of the amphiphilic film. Generally, the amphiphilic film would like to attain the spontaneous curvature, which is normally affected by nature of the surfactant and composition of the system [5, 6].
In the present report (Fig. S1A), CTAB is used as tuning parameter to change the spontaneous curvature of the interfacial film. The surfactant film is convex toward oil with increasing proportion of CTAB which leads to the formation of w/o microemulsion droplets [5-7]. The formation of microemulsion is dependent on composition of the mixed surfactants and is sigmoidal in nature with rapid increase of single phase microemulsion zone, 1ϕ (%). The process of addition of CTAB is cooperative in nature. The threshold values of mixed surfactants composition (Brij-58: CTAB, w/w) towardthe formation of single phase microemulsion zone, 1ϕ are obtained in terms of Sigmoidal-Boltzmann equation and the values are 3.68 ± 0.26 (Hp) and 3.73 ± 0.35 (Dc), respectively. The predominance of w/o microemulsion formation over o/w was identified from the overall scenario of different phase diagrams at different compositions of Brij-58 and CTAB (Fig. S1). Kahlweit et al. [5] reported that the addition of SDS reduces the amount of nonionic $C_iE_j$needed to form a single phase microemulsion from equal volumes of water and alkanes. Silas et al. [6] also reported that the addition of DDAB increases the efficiency of nonionic surfactants, n-alkyl polyglycol ethers (C_iE_j) to form microemulsions with decane.

However, when one analyses the results in terms of the variation of % area under the clear region with the variation of oil chain length, it can be observed from Fig. S1Athat % area under the clear region is higher for Hp stabilized systems compared to Dc stabilized systems. Oil can influence the property of an interface through a surfactant chain-oil interaction. Strong interaction leads to a large penetration of oil molecules into the surfactant chain layer (solvation), which further increases the rigidity as well as curvature (or, packing ratio, v/al) of the interface [8]. As a result of that, shorter chain Hp produces larger single phase microemulsion zone than Dc. Similar observation was reported earlier by Mitra and Paul [9] for water/C_{16}TAB or Brij-58/Bu/Hp or Dc microemulsion systems.

3.Dye solubilization experiment

In the present report, dye solubilization experiment has been performedat single (Brij-58) as well as mixed (Brij-58 and CTAB) surfactant microemulsion at low and rich compositions of cationic surfactant (CTAB). According to Shah and coworkers [8, 10], solubilization process and consequently the phase separation in such systems is limited by two opposing factors, viz. the critical radius of droplets (R_c), due to the result of attractive interaction among the droplets and the radius of spontaneous curvature (R_0) as the result of curvature effect. The curvature effect is related to the cohesive force between the hydrocarbon chains of amphiphiles at the interface as well as to the rigidity of the interface. For single Brij-58 stabilized system and mixed Brij-58/CTAB system with Brij-58 rich composition, it has been found that after complete phase separation (upon addition of excess water), addition of an oil soluble dye Sudan IV made both the phases to turn red, whereas addition of a water soluble dye Eosin Blue turned the lower phase violet keeping the upper phase colorless. This indicates that the upper phase is a pure oil phase in equilibrium with the lower microemulsion phase (Winsor I type). Thus for these systems phase separation can be assumed to be governed by the interdroplet interaction phenomenon (R_c) [10, 11]. On the other hand, after complete phase separation of single CTAB stabilized system and mixed Brij-58/CTAB systems with CTAB rich composition, when Sudan IV was added into it, the upper phase became intense red, whereas the lower phase remained colorless. But, upon addition of Eosin Blue, the lower phase became intensely violet and the upper phase faintly violet. This study points out to the fact that the lower phase is a pure aqueous phase in equilibrium with an upper microemulsion phase (Winsor II type). Thus the phase separation can be assumed to be governed by the curvature effect (R_o) [10, 11]. Hence in the solubilization capacity versus mixed surfactant composition profile (Fig. 1), the ascending curve can be identified as the R_c branch (interdroplet interaction branch), whereas the descending curve as the R_0 branch (the curvature branch).

4. Conductivity measurements

It is known that electrical conductivity measurements can be used to predict qualitatively the interaction between the droplets and thus stability of microemulsion. For example, appearance of an electrical percolation process indicates the existence of large attractive interaction between droplets [12-14]. In this section, an attempt has been made to correlate the maximum water solubilization with percolation of conductance in mixed microemulsion systems to underline the microstructure of these mixed surfactant microemulsions. If the droplets are of non-interacting hard sphere type, no significant increase in conductance occurs with increasing water content at constant temperature or with increase in temperature at fixed water content. But if the interfaces of the droplets are fluid enough to coalesce during these collisions followed by material exchange and fusion, a sharp rise in conductance is evidenced [13]. In the present investigation, conductance studies have been carried out for mixed surfactant microemulsion systems wherein solubilization maxima (in the vicinity of equimolar composition i.e., at Brij-58: CTAB = 2:3 and

3:2, w/w) are observed. The samples from both sides of the corresponding maxima, i.e., from the ascending branches and the descending branches are chosen.

The conductivity of mixed water/Brij-58/CTAB/Pn/Hp or Dc microemulsion systems at different compositions (Brij-58: CTAB = 5:0; 4:1; 3:2; 2:3; 1:4; 0:5, w/w) [S: CS = 1:2 (w/w)] at 303K as a function of wt% of water has been determined and depicted in Figs. S2A-S2F. Samples chosen from the ascending branch (i.e., at Brij-58: CTAB = 5:0→2:3, w/w) exhibit a nonlinear sharp enhancement in conductivity with the addition of water, which signifies the volume-induced percolation in conductance (Figs. S2A-S2D). The critical value for sharp enhancement in conductivity with the addition water is considered as volume-induced percolation threshold (ϕ_p). It is well known that, percolation of conductance study extracts information about the nature of interaction among the droplets in w/o microemulsions/reverse micellar systems [11, 13]. Such percolation in the present systems (i.e., at ascending branch of Fig. 1) shows that the interface of the droplets are fluid enough to coalesce during the collisions followed by material exchange and fusion. As a result, a sharp rise in conductance is evidenced. Further, it is evident that ϕ_p increases (i.e., percolation process is retarded) with decrease in content of Brij-58 or increase in content of CTAB. On the other hand, no sharp enhancement in conductivity vis-à-vis percolation phenomenon is observed in the descending branch of the solubilization maximum (i.e., at Brij-58: CTAB = 1:4→0:5, w/w) (Figs. S2E-S2F). Here, the overall increase in conductivity with increase in water content for the systems chosen from descending branch (R_0) can be explained in the following manner. Initially, the amount of dispersed droplet increases with the addition of water while its droplet size increased slightly. The increase of collision probability enhances the conductivity of microemulsion. With further addition of water, the density of surfactant molecules in the interfacial film decreases due to the expansion of dispersed droplets. The aforesaid two influences make the interfacial film more unconsolidated which is beneficial to the increase of conductivity [15].

At composition of single Brij-58 (Brij-58: CTAB = 5:0, w/w), the microemulsion systems (single Brij-58-derived) exhibit percolation phenomenon in both oils (Fig. S2A). This is possibly due to the progressive increase in the hydration of the ethylene oxide moieties of the head group of the surfactant, rendering a better conducting entity that possibly exists in rapid equilibrium with reverse micelles. It can be concluded that beyond ϕ_p = 0.82 (vide.Table S2), a network of conductive channels exists, which corresponds to the formation of water cylinders or channels in an oil phase due to the attractive interaction between the spherical micro droplets of the water phase in the w/o microemulsion [12]. Similar result was also reported by Mehta et al. [12] for water/Brij-96/alcohol (n_2-n_6)/EO microemulsions systems.

At a composition of (Brij-58: CTAB = 0:5, w/w) i.e., single CTAB-derived microemulsion systems do not exhibit percolation phenomenon in both oils (Fig. S2F). In this system, CTAB molecule dissociates into cation [$N(CH_3)_3^+$] and counter-ion (Br^-) in the water pool. The hydrophobic part associated with polar head group (viz. [$N(CH_3)_3^+$] and C_{16} hydrocarbon chain) can combine with water or oil molecule accordingly and form a compact interfacial film. Therefore, the counter ions are difficult to cross the interfacial film during the thermal motion process [15].

A bell-shaped conductivity profile with flattened maxima is obtained (Fig. S2F), as reported earlier using cationic surfactant, CTAB/Pn/Hx/water [16] and anionic surfactant, AOT/i-Oc/water [17]. The low initial conductivity of the system is attributed to the negligible interactions between the isolated “hard sphere like” water globules dispersed in the continuous oil medium [18]. With gradual addition of water, dispersed water droplets grow, and the enhanced attractive interaction between them leads to the formation of water clusters. The increase in the conductivity in oil-rich microemulsions is thus derived from an increase in the dispersed droplet sizes and the enhanced attractive interactions between the droplets [19]. At the threshold composition, such clustering leads to the formation of a bicontinuous structure wherein the infinite radius of curvature of the

aggregate results in the maximum conductivity of the system. In our study, the maximum of conductivity occurs at ϕ = 0.22-0.27 for Hp and Dc, wherein a bicontinuous microemulsion is realized. Further addition of water causes a decrease in conductivity, indicating that water, which is the least viscous component of the microemulsion system, becomes the outer phase, eventually forming o/w microemulsions. In this aqueous-rich region, conductivity gradually decreases expectedly due to dilution effect of the o/w microemulsion droplets [20].

The influence of composition of mixed surfactant (Brij-58/CTAB) (4:1, 3:2, 2:3 and 1:4, w/w) on the conductivity in both oils has been presented in Figs. 3A-3D. In the mixed compositions, the interfacial film is composed of hydrocarbon tails of surfactant molecules, cosurfactant molecules, oil molecules and the water pool is composed of counter ions adsorbed by the ionic head group, water molecules combined with the POE chains [15]. The characteristic features of the two types of surfactants (i.e., cationic and non-ionic) are likely to produce the mixed interfacial film a special structure. Brij-58 molecules are electropositive (due to formation of hydronium ions), as a result of their interaction between POE chains and water [15]. Similarly, CTAB molecules dissociates into halide counter ions (Br^-) and cations [$N(CH_3)_3^+$]. When the two surfactants are mixed in the interfacial film, the electrostatic repulsion decreases the compactness of the interfacial film and the transportation of charge becomes easier. Moreover, the composition of the interfacial film is special as well, because of monomer mole fractions of the two surfactants in mixed film and micelles are different from those in the bulk phase. Subsequently, such a special type of composition is beneficial to improve the flexibility of the surfactant film which is an important factor for the formation of reverse microemulsion [21]. All these factors, as mentioned above, made the mixed Brij-58/CTAB microemulsion systems percolative up to certain compositions (i.e., Brij-58: CTAB = 4:1→2:3, w/w), beyond which no such percolation was observed. This might be explained in the following manner. It was reported that with increase in counter ion concentration due to progressive addition of CTAB, diminishes the effective polar head area of the surfactants by screening the electrostatic repulsion, which makes surfactant membranes more rigid and decreases the attractive interactions among the droplet [13, 22]. Hence, it can be concluded that the interaction between the two surfactants can increase the conductivity of microemulsion to an ideal level which is desired in the direct application of electrochemistry [15].

The mechanism of percolation is governed by two approaches,static and dynamic [12]. The concept of percolation is governed by scaling laws as given in the following equation:

$$\sigma = P (\phi - \phi_p)^t \quad \text{(S9)}$$

where, σ is the specific conductance, ϕ is the weight fractions of water, ϕ_p is the threshold value. P is a free parameter and t is a critical component. As per percolation theory, the value of t > 1.2 explicatesthe dynamic nature of the microemulsion system [23].Here the average value of critical exponent (t) (= 0.86) is 28% lower than that of 1.2. The constants and exponents predicted in theory were based on systems consisting of solid conductors and insulators [24]. The soft systems like microemulsion are intrinsically different in conducting behavior, which make the critical exponent (t) different from 1.2. However value of critical exponent (t) depends on the softness of microemulsion systems [3]. The values of t and ϕ_p are given in Table S2 with variation in mixed surfactant compositions.

It is also evident from Table S2 that the percolation threshold (ϕ_p) gradually increases with increased CTAB proportion (= 5:0→2:3, w/w). Addition of CTAB decreases the droplet radius by increasing the critical packing parameter (CPP), which in turn hinder the droplet coalescence that limits the solubilization capacity [13]. However, the values of percolation threshold (ϕ_p) are found to be slightly lower in Dc continuum than that of Hp (Table S2). It was reported that the process of coalescence of droplets followed by exchange of materials is accompanied by oil removal from the interface, and the interfacial fluidity may increase with increasing ease of oil

removal [25]. The absorption of oil molecules into the interface increases significantly for oils with smaller chain length (herein Hp), which in turn hinders the droplet coalescence process. On the other hand, for oils with larger chain length (herein, Dc), or penetration into the interface is reduced and hence removal of oil molecules from the interface duringcollision is eased. So the percolation phenomenon is facilitatedfor Dc. Similar studies of percolation phenomenon have already been reported for single (ionic or non-ionic) and mixed surfactant (ionic/nonionic) microemulsion systems in absence and presence of cosurfactant [3, 11-13, 26].

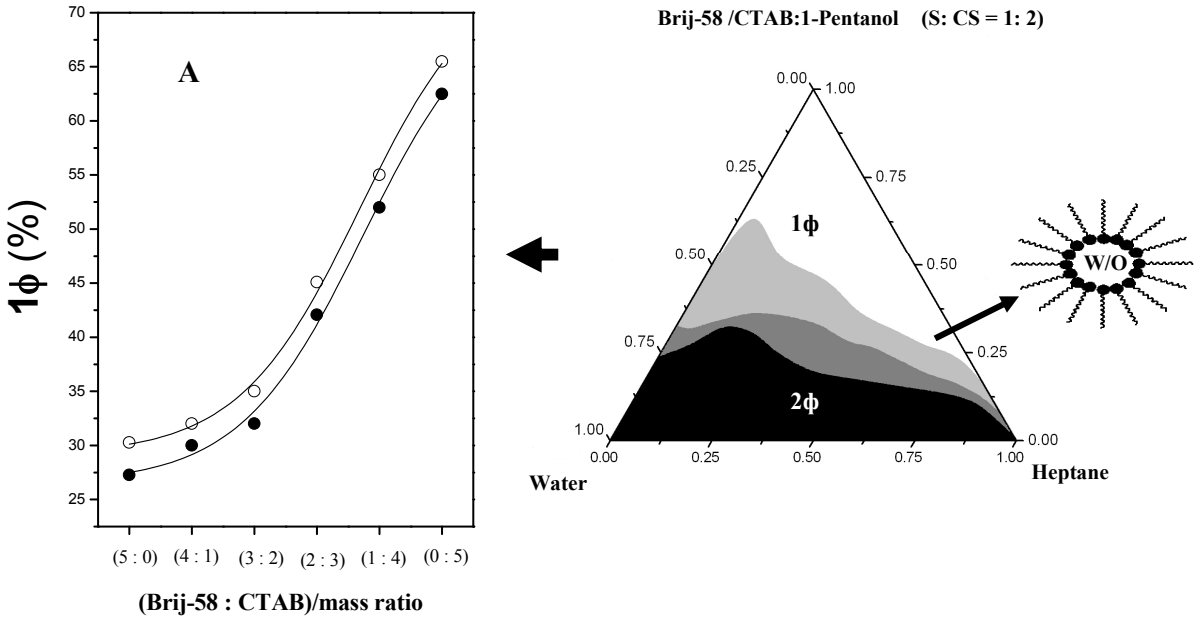

Fig. S1. Pseudo-ternary phase diagram of water/Brij-58: CTAB/Pn/Hp at different mass ratios of mixed surfactant at 303K. S and CoS mass ratio = 1: 2. Area marks: unshaded, microemulsion zone (1ϕ); shaded, turbid zone (2ϕ) [light gray, 5: 0; dark gray, 2: 3 and black, 0: 5 mixing ratio of Brij-58 and CTAB, respectively]. **Fig. A** represents % of microemulsion zone (1ϕ) against mixed surfactant mass ratio (open square: heptane, filled square: decane).

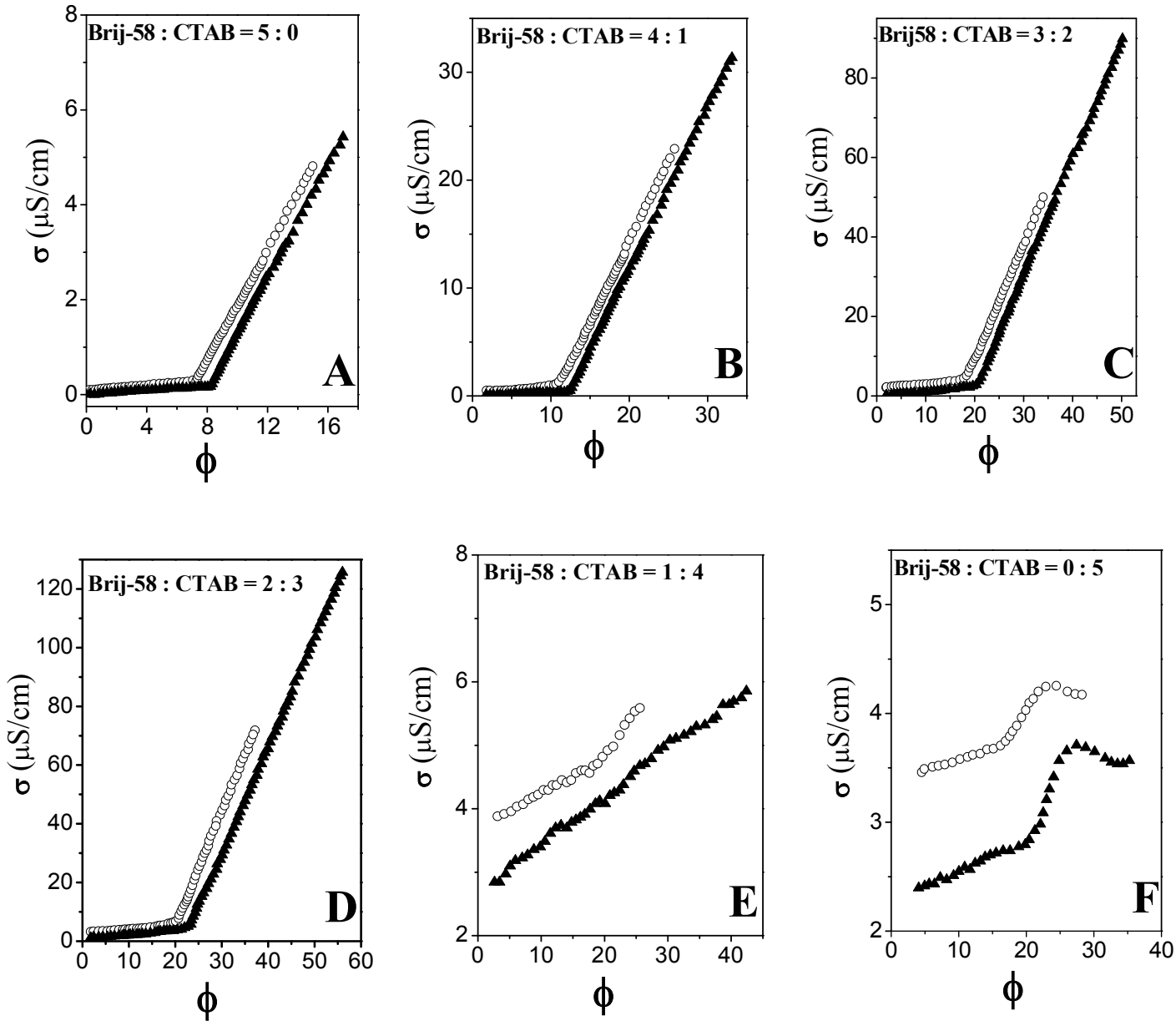

Fig. S2. Dependence of electrical conductivity (σ) on weight fraction of water (ϕ) for water/Brij-58: CTAB/1-pentanol/heptane (decane) microemulsions with six different mass ratios of mixed surfactant [at constant S: CS = 1:2 (w/w)] at a fixed temperature of 303K (Hp: filled triangle and Dc: open circle).

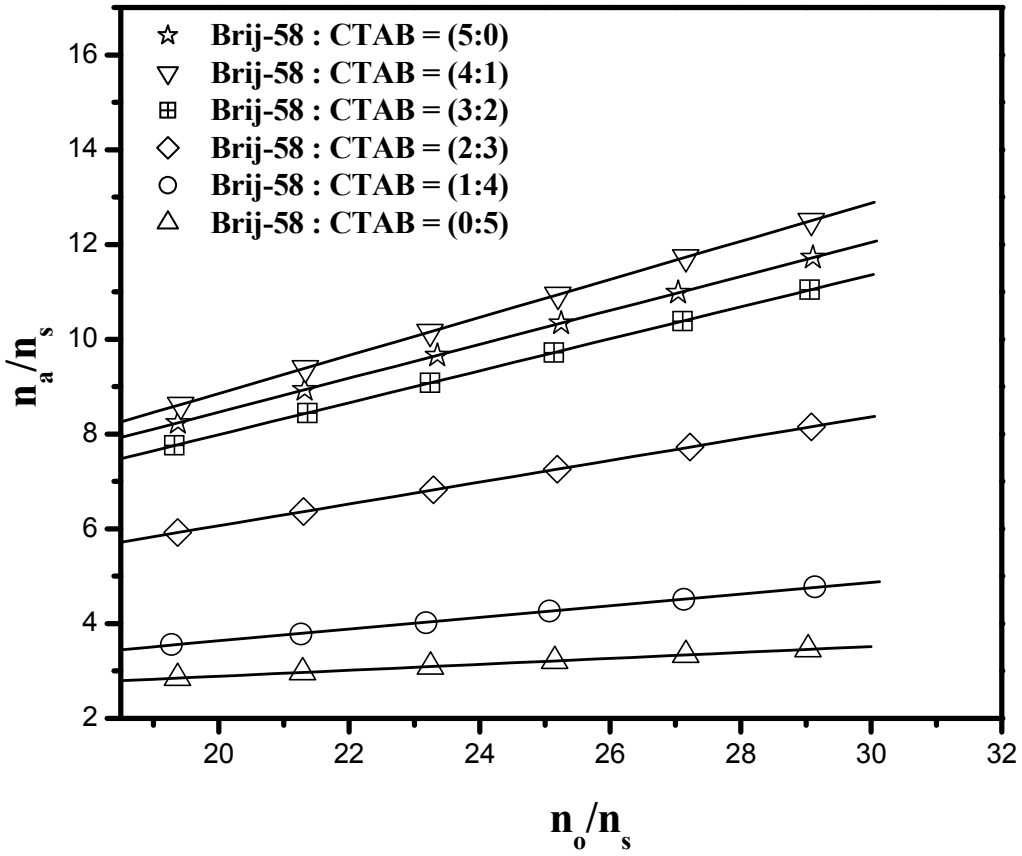

Fig. S3. Plots of n_a / n_s vs. n_0 / n_s for w/o microemulsion systems comprising water (2.75×10^{-2} mol), mixed surfactant (5×10^{-4}mol) and heptane (2 ml) stabilized by 1-pentanol with different composition of mixed surfactant at constant temperature (303K).

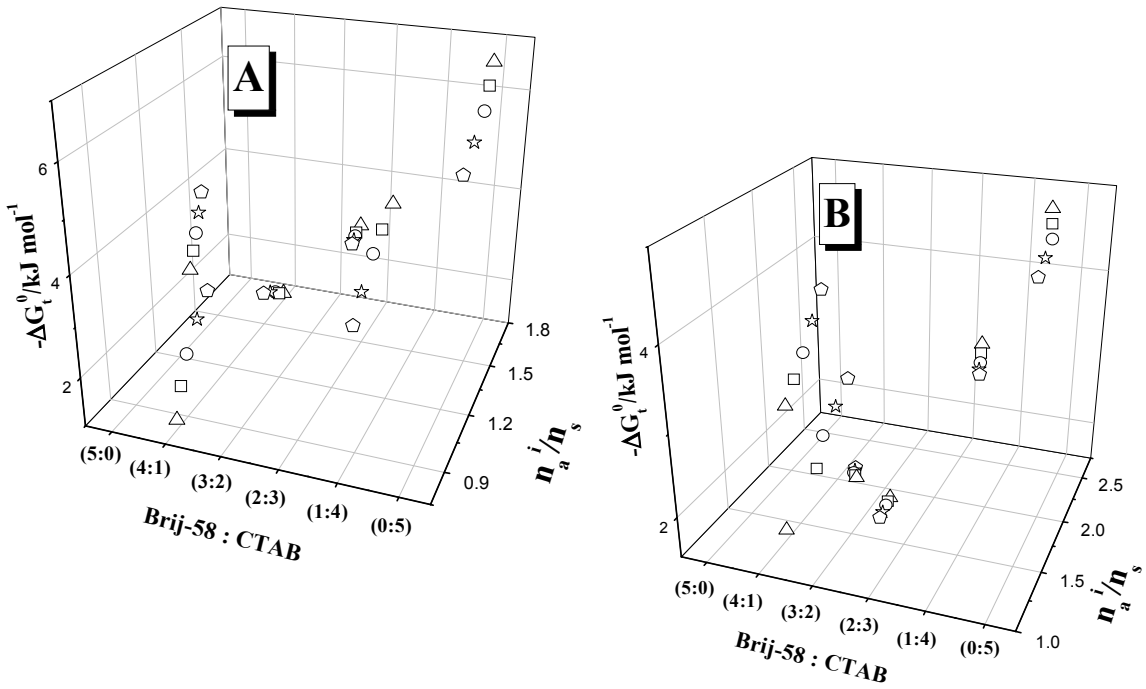

Fig. S4. Plot of n_a^i/n_s and $-\Delta G^0_t$ vs. different mass ratios of mixed surfactant (Brij-58 and CTAB) for w/o microemulsion systems comprising 5×10^{-4}mol of total mixed surfactant, 2.75×10^{-2} mol water, 2 ml of heptane (**Plot: A**) and decane (**Plot: B**) stabilized by 1-pentanol at five different temperatures [303K (open triangle), 308K (open square), 313K (open circle), 318K (open star), 323K (open pentagon)].

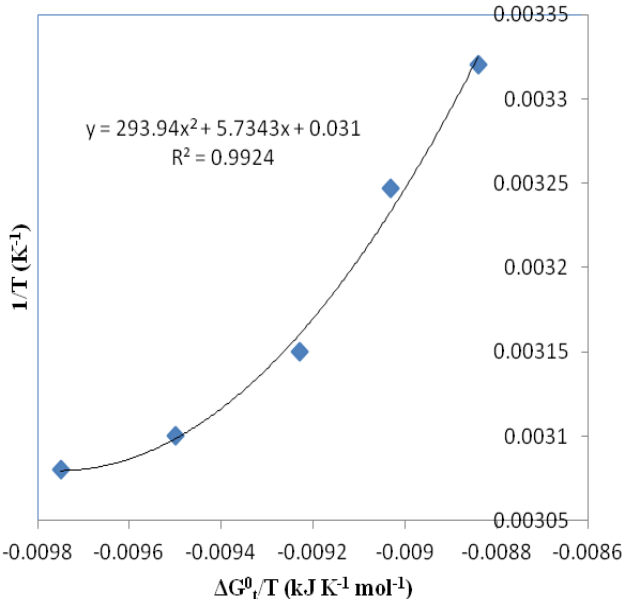

Fig. S5. Plot of $(\Delta G^0_t/T)$ vs. (1/T) for water/Brij-58/CTAB/1-pentanol/Hp system at fixed Brij-58: CTAB (= 3:2, w/w) and water content (2.75×10^{-2}mol).

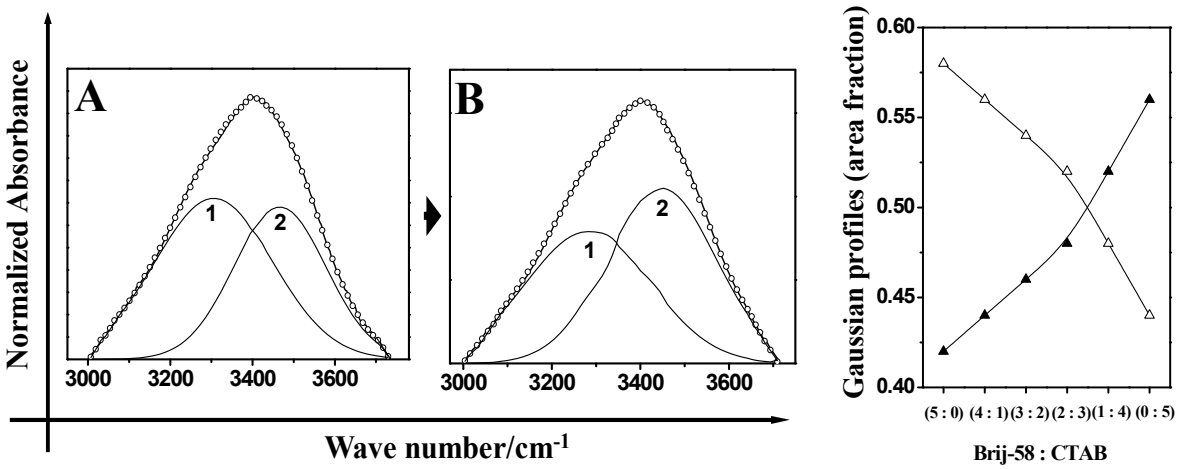

Fig. S6. Representative FTIR spectra of O-H band for mixed surfactant (Brij-58: CTAB) w/o microemulsion system stabilized in Hp at fixed water content (2.75×10^{-2} mol), surfactant and cosurfactant mass ratio (1:2) and temperature (303K) [A: pure nonionic (Brij-58: CTAB = 5:0, w/w); B: near middle range composition (Brij-58: CTAB = 2:3, w/w)]. Specification: Experimental spectra overall fitted point (open circle) and deconvoluted curves (*1: bulk water; 2: bound water*). The variation of Gaussian profiles (area fraction) of the normalized spectra of different water species (bulk water: open triangle; bound water: filled triangle) as a function of composition (Brij-58: CTAB = 5:0→0:5, w/w).

Table S1. Compensation temperature (T_{comp}) from the plot of ΔH^0_t against ΔS^0_t for mixed surfactant microemulsion systems.

System	Experimental Temperature (K)	303	308	313	318	323
Water/Brij-58 /CTAB/Pn/Hp (Dc)	Compensation Temperature (K)	303.1 (0.9999)[a]	308.1 (0.9999)	313.1 (0.9999)	318.1 (0.9999)	323.1 (0.9999)

[a] Values of correlation of coefficients.

Table S2. Percolation threshold volume fraction and scaling parameters for the formation of w/o mixed microemulsions at different mass ratios of mixed surfactant and fixed temperature (303K) [a]

System: water/Brij-58/CTAB/Pn/Hp (Dc)

Brij-58 : CTAB	$_{10}\phi_p$	t
5 : 0	0.82 (0.73)	0.59 ± 0.01 (0.75 ± 0.02)
4 : 1	1.26 (1.10)	0.80 ± 0.01 (0.79 ± 0.02)
3 : 2	2.09 (1.82)	1.09 ± 0.01 (1.08 ± 0.01)
2 : 3	2.30 (2.07)	0.95 ± 0.02 (0.87 ± 0.01)

[a]All the mixed microemulsion systems are formed using constant amount of mixed surfactant (5×10^{-4}mol), water (2.75×10^{-2}mol) and oil (2 ml).

References

[1] E. Abuin, E. Lissi, K. Olivares, J. Colloid Interface Sci. 276 (2004) 208.

[2] O. Zheng, J-X. Zhao, H. Yan, S-K. Gao, J. Colloid Interface Sci. 310 (2007) 331.

[3] K. Maiti, I. Chakraborty, S.C. Bhattacharya, A.K. Panda, S.P. Moulik, J. Phys. Chem. B 111 (2007) 14175.

[4] D. Mitra, I. Chakraborty, S.C. Bhattacharya, S.P. Moulik, S. Roy, D. Das, P.K. Das, J. Phys. Chem. B 110 (2006) 11314.

[5] M. Kahlweit, B. Faulhaber, G. Busse, Langmuir 10 (1994) 2528.

[6] J.A. Silas, E.W. Kaler, J. Colloid Interface Sci. 243 (2001) 248.

[7] C. von Corswant, S. Engström, O. Söderman, Langmuir 13 (1997) 5061.

[8] R. Leung, D.O. Shah, J. Colloid Interface Sci. 120 (1987) 320; 330.

[9] R.K. Mitra, B.K. Paul, S.P. Moulik, J. Colloid Interface Sci. 300 (2006) 755.

[10] M.J. Hou, D.O. Shah, Langmuir 3 (1987) 1086.

[11] R.K. Mitra, B.K. Paul, Colloids Surf. A 255 (2005) 165.

[12] S.K. Mehta, G. Kaur, R. Mutneja, K.K. Bhasin, J. Colloid Interface Sci. 338 (2009) 542.

[13] B.K. Paul, R.K. Mitra, J. Colloid Interface Sci. 288 (2005) 261.

[14] D. Liu, J. Ma, H. Cheng, Z. Zhao, Colloids Surf. A 135 (1998) 157.

[15] J. Hu, H. Zhou, G. Zhang, Y. Cui, L. Huang, Y. Xu, J. Chen, Y. Kuang, J. Appl. Electrochem. 40 (2010) 2033.

[16] M. Giustini, G. Palazzo, G. Colafemmina, M.D. Monica, M. Giomini, A. Ceglie, J. Phys. Chem. 100 (1996) 3190.

[17] H.F. Eicke, M. Borkovec, B. Das-Gupta, J. Phys. Chem. 93 (1989) 314.

[18] M. Gradzielski, H. Hoffman, In Handbook of Microemulsion Science and Technology, P. Kumar, K. L. Mittal (Eds.), Marcel Dekker: New York, 1999, pp 161.

[19] Z. Saidi, C. Mathew, J. Peyrelasse, C. Boned, Phys. Rev. A 42 (1990) 872.

[20] R. Saha, S. Rakshit, R.K. Mitra, S.K. Pal, Langmuir 28 (2012) 8309.

[21] S. Lamaallam, H. Bataller, C. Dicharry, J. Lachaise, Colloids Surf. A 270-271 (2005) 44.

[22] C. Rodríguez, D. P. Acharya, S. Hinata, M. Ishitobi, H. Kunieda, J. Colloid Interface Sci. 262 (2003) 500.

[23] B. Lagourette, J. Peyrelasse, C. Boned, M. Clausse, Nature 281 (1979) 60.

[24] J.C. Maxwell, In Electricity and Magnetism, 3rd ed., Oxford University, London 1982.

[25] B. Lemaire, P. Bothorel, D. Roux, J. Phys. Chem. 87 (1983) 1023.

[26] S. Paul, S. Bisal, S.P. Moulik, J. Phys. Chem. 96 (1992) 896.